Inflation, Extension, Torsion and Shearing of an Inhomogeneous Compressible Elastic Right Circular Annular Cylinder

U. Saravanan and K. R. Rajagopal

Mathematics and Mechanics of Solids 2005 10: 603
DOI: 10.1177/1081286505036422

Inflation, Extension, Torsion and Shearing of an Inhomogeneous Compressible Elastic Right Circular Annular Cylinder

U. SARAVANAN
K. R. RAJAGOPAL
Department of Mechanical Engineering, Texas A&M University, College Station, Texas 77843-3123, USA

(Received 25 November 2002; accepted 23 May 2003)

Dedicated to Professor M. Hayes on his 65th birthday.

Abstract: We study the inflation, extension, torsion and shearing of an isotropic inhomogeneous compressible annular right circular cylinder. Current approaches to homogenization that appeal to an equivalence in the stored energies could lead to serious errors in the estimate for stresses in a inhomogeneous body as stresses depend on the derivatives of the stored energy with respect to the deformation gradient. This is a serious drawback as many a time failures are determined by the stresses. The study demonstrates that, in particular, great caution should be exercised in homogenization, especially if an inhomogeneous body is to be approximated by a homogeneous body belonging to the same class. Comparison of local measures, such as stresses, reveal that their values in the case of the inhomogeneous body and its homogeneous counterpart can be both qualitatively and quantitatively far apart. Even the differences in global measures like the axial load, torque, etc., are found to be significant between the inhomogeneous body and its homogeneous counterpart. It is also shown that the material parameters characterizing the homogenous approximation gleaned from correlations from different experiments, performed on the same inhomogeneous body, can be quite different.

Key Words: inhomogeneous bodies, equivalent stored energy, homogenization, compressible body, isotropic body

1. INTRODUCTION

Advances in material science have led to the engineering of many bodies such as polymer and metal matrix composites and metallic alloys which are inhomogeneous. Also, most biological bodies like arteries, tendons, ligaments, etc., are inhomogeneous. Efficient design and optimal choice of the constituents has resulted in increased safety, as well as cost savings and this in turn has led to increased use of composites. However, such structures do fail, and the cause for the failure is still poorly understood. In the case of biological bodies, it is imperative to understand the role of inhomogeneities if one is to comprehend the growth and adaptation process of bodies suffering various pathologies like hypertension and aneurysms. These and many other technologically important problems have kindled the interest in the study of the response of inhomogeneous bodies in recent years.

Two material points $\mathbf{P}_1, \mathbf{P}_2 \in \mathcal{B}$ are said to be materially uniform (see Truesdell and Noll [1]), when attention is restricted to purely mechanical processes (i.e. we do not consider the body's thermal, electro-magnetic or other responses), if there exist two placers κ_1 and

Mathematics and Mechanics of Solids **10:** 603–650, 2005 DOI: 10.1177/1081286505036422

κ_2 such that there exist neighborhoods $N_{\mathbf{X}_1}$ of $\mathbf{X}_1 = \kappa_1(\mathbf{P}_1)$ and $N_{\mathbf{X}_2}$ of $\mathbf{X}_2 = \kappa_2(\mathbf{P}_2)$ that are indistinguishable with respect to their mechanical response. A body, $\mathcal{B}$, is said to be homogeneous if all the material points are materially uniform with respect to a single placement. A body that is not homogeneous is said to be inhomogeneous.

A deformation is said to be homogeneous if in a Cartesian coordinate system, the matrix components of the deformation gradient ($\mathbf{F}_{\kappa_R}$) has constant entries. Thus, in a homogeneous deformation straight lines remain straight lines after deforming. A deformation that is not homogeneous is said to be inhomogeneous. Hence, a homogeneous body can deform homogeneously or inhomogeneously as can an inhomogeneous body.

Ericksen [2] showed that the only deformations possible in every member of the class of isotropic homogeneous compressible elastic bodies are homogeneous deformations. Hence, inhomogeneous deformations of inhomogeneous isotropic compressible elastic bodies have to be studied for specific forms of the stored energy function.

Here we consider bodies which have a stored energy of the form proposed by Blatz and Ko [3]. The response of homogeneous Blatz–Ko bodies (i.e. bodies whose stored energy is given by the form proposed by Blatz and Ko [3]) to homogeneous deformations has been studied in some detail (see for example [4, 5, 6]). A variety of analytical and numerical solutions have been obtained for special sub-classes of Blatz–Ko bodies when the deformation is inhomogeneous. Chung et al. [7] obtained analytical solutions for the inflation of a cylinder. Carroll and Horgan [8] obtained analytical solutions for the pure torsion of a circular cylinder and also deformations analogous to controllable deformations for incompressible bodies. Polignone and Horgan [9, 10, 11] explored the forms of the stored energy functions that support isochoric deformations corresponding to torsion, longitudinal or circumferential shear and found special classes of stored energy functions that admit such solutions. Mioduchowski and Haddow [12] studied the axial and torsional shearing of a circular cylindrical tube, Zidi [13, 14] studied torsion and circumferential shearing, torsion and telescopic shearing of compressible anisotropic tubes and Zidi [15] studied torsion, circumferential and telescopic shearing of compressible anisotropic tubes.

Here we study the combined inflation, extension, torsion, circumferential and longitudinal shearing of inhomogeneous, compressible bodies. We use a semi-analytical solution scheme that can be used for a large choice of stored energy functions. We illustrate the efficacy of the method within the context of the Blatz–Ko stored energy function.

In the study of composites, polycrystals, bodies with voids or cracks and many other bodies, it is common to homogenize the inhomogeneous body and work with the homogenized approximation. The purpose here is not to present the homogenization procedure or obtain bounds for errors if and when possible, but to explore the appropriateness of homogenization that appeals to the equivalence of stored energies, by comparing the solutions obtained by solving identical boundary value problems (BVPs) for both the inhomogeneous body and its homogeneous approximation. From a practical standpoint, while carrying out such a homogenization, we have to

(1) ensure that the actual inhomogeneous body will not fail, when subject to external loading at which the corresponding approximate homogenized model predicts that the body would not do so (or vice versa);
(2) obtain a good estimate for the force or traction required to enforce a displacement boundary condition (or vice versa).

Hill [16] was one of the early investigators to consider the homogenization of heterogeneous bodies. Much of the research that has followed this has been concerned with homogenization such that the total stored energy of the inhomogeneous body and its homogeneous counterpart are the same for a given BVP, or they are concerned with obtaining bounds for material parameters for the homogeneous approximation. Other than the study, by Imam [18] of a problem analogous to the one studied by Eshelby [17] most other studies in finite elasticity concerns with obtaining estimates. Of course, it might be relevant, in certain cases, for both the inhomogeneous body and its homogeneous counterpart to have the same total stored energy, but the question is whether this assumption will help the engineer satisfactorily answer all the issues of interest, for example develop a reasonable failure criterion. Here we show that most such homogenization procedures cannot lead to the development of a meaningful criterion. That is, equivalence of stored energy does not ensure that the estimate for stresses or tractions will be robust. These differences arise because the quantities that are of interest are related to the gradient of the stored energy.

Bolzon [19], using the same methodology as Hill [16], homogenized the Blatz–Ko model, using numerical methods. He studied the response of a sheet with **a** circular void in the center and sought to obtain a homogeneous model that fills in the void. He concluded that the inhomogeneous Blatz–Ko model cannot be approximated by a homogeneous Blatz–Ko model.

Let γ denote some generic material parameter, which varies over the body. Then, we could define a mean value for γ as

$$\gamma_{mean} = \frac{\int_V \gamma(\mathbf{X})\,\mathrm{d}V}{\int_V \mathrm{d}V}, \tag{1}$$

We then define that two inhomogeneous bodies are equivalent if the mean of each of their material parameter(s) is the same. By equivalent we do not mean that their mechanical response will be the same or similar. While two inhomogeneous bodies can have the same mean shear modulus their response could be markedly different. This depends on the inhomogeneity and on the deformation under consideration. This will become apparent during the course of this study. We could also introduce the mean by introducing weight functions in the integral (1).

Consistent with the findings of Saravanan and Rajagopal [20, 21] we show that the above average has no relevance to the constant value for the property, even if the inhomogeneity is very "mild" (a body with holes in it or an inclusion that has markedly different properties, is not a mildly inhomogeneous body). This is of course not in the least surprising.

Suppose we perform an experiment in which we axially pull an inhomogeneous, isotropic, compressible elastic right circular cylinder and use a constant value γ_{exp}^{Ax-Ext} such that the axial load required to engender a certain stretch correlates well with the experiment. Then, we find that $\gamma_{exp}^{Ax-Ext} \neq \gamma_{mean}$, in general. Also, the constant value obtained from correlating with different experiments, namely γ_{exp}^{Pr-Inf} for pressurizing and inflating, γ_{exp}^{Ax-Ext} for axial extension, are different. For a given inhomogeneity, depending on the specific BVP, γ_{exp} could vary by as much as 1800% in the correlations from different experiments. Such large variations suggest the futility and inadequacy in obtaining bounds for these material parameters using the criteria of equivalent moduli, as they cannot be tight. Of course, here we have assumed that the stored energy of the homogeneous approximation belongs

to the same class as that of the inhomogeneous body. We might of course need to model an inhomogeneous body comprised of homogeneous bodies of a certain class by a homogenized model of a different class, i.e. a body comprised of different Blatz–Ko bodies would be approximated by a homogenized body that is not a Blatz–Ko body. In fact, this would indeed be the case. However, if the inhomogeneity is "mild", i.e. if the body is made up of Blatz–Ko bodies whose material properties are close to one another, we would be tempted to model the inhomogeneous body as an equivalent homogeneous Blatz–Ko model. In fact, many studies make such an assumption. Few rigorous studies concern non-linear elastic inhomogeneous solids undergoing large deformations. Irrespective of the homogenization procedure, if such a model is arrived at based on energy considerations it will not lead to models that predict the stress accurately. It has been suggested erroneously that one could approximate an inhomogeneous isotropic body as a homogeneous anisotropic body (see for example [22]). However, it should be borne in mind that material symmetry concerns response at a material point and inhomogeneity is associated with the response at different material points.

We study the variation of these constant values, γ_{exp} for different types of departures from the mean, i.e. we examine if the results obtained are significantly different for a sinusoidal variation versus a piecewise constant or linear variation, provided the mean value is the same. We find that depending on the inhomogeneity, γ_{exp}^{Tr-Twt}, the constant obtained from correlating the torque required to engender a given twist for a specific stored energy function could vary by as much as 360%, indicating the importance of knowing the actual inhomogeneity. Thus, the parameter γ_{exp} will be different for different inhomogeneous bodies even though they are in some sense equivalent.

When we focus our attention to local quantities such as the stress, we once again reaffirm the observation of Saravanan and Rajagopal [20,21] that even the sense of the stresses cannot be captured correctly by the homogenized approximation. Thus, even if homogenization is reasonable for the global response of the body, it is quite inappropriate when one is interested in determining the failure of the body.

The arrangement of the paper is as follows. In Section 2 we introduce the basic kinematical quantities and follow this in Section 3 with a discussion of the stored energy function that is considered in this study. In Section 4 we introduce the various types of inhomogeneities considered. In the next section we introduce the specific deformations that are to be studied and outline the semi-analytical scheme to solve the BVP. In Section 6 we obtain γ_{exp} from various correlations. In Section 7 we present a few interesting results concerning the distribution of stresses in inhomogeneous compressible solids vis-à-vis the homogenized body. This is followed by a very brief account of the response of homogeneous compressible solids.

2. KINEMATICS

Let $\mathbf{X} \in \kappa_R(\mathcal{B})$ denote a typical particle belonging to the natural reference configuration $\kappa_R(\mathcal{B})$ of the body, and let $\mathbf{x} \in \kappa_t(\mathcal{B})$ denote the position occupied by $\mathbf{X}$ at time t in the configuration $\kappa_t(\mathcal{B})$. The motion of the body is defined through the mapping χ_{κ_R} that is one-to-one for each $t \in \mathsf{R}$:

$$\mathbf{x} = \chi_{\kappa R}(\mathbf{X}, t). \tag{2}$$

We shall assume that the motion is sufficiently smooth to render all the derivatives that follow to be meaningful. The deformation gradient $\mathbf{F}_{\kappa R}$ is defined through

$$\mathbf{F}_{\kappa R} = \frac{\partial \chi_{\kappa R}}{\partial \mathbf{X}}, \tag{3}$$

and the Cauchy–Green stretch tensors, $\mathbf{B}_{\kappa R}$ and $\mathbf{C}_{\kappa R}$, are defined through

$$\mathbf{B}_{\kappa R} = \mathbf{F}_{\kappa R}\,\mathbf{F}_{\kappa R}^{T}, \tag{4}$$

$$\mathbf{C}_{\kappa R} = \mathbf{F}_{\kappa R}^{T}\,\mathbf{F}_{\kappa R}. \tag{5}$$

The principal invariants of any second-order tensor $\mathbf{A}$ are defined through

$$I_1 = \operatorname{tr}\mathbf{A}, \quad I_2 = \frac{1}{2}[(\operatorname{tr}\mathbf{A})^2 - \operatorname{tr}\mathbf{A}^2], \quad I_3 = \det\mathbf{A}. \tag{6}$$

We find it convenient to express some of the results in terms of the invariants

$$J_1 = I_1, \quad J_2 = \frac{I_2}{I_3} = \operatorname{tr}\left(\mathbf{A}^{-1}\right), \quad J_3 = I_3^{1/2}. \tag{7}$$

These kinematical quantities are sufficient for our purpose.

3. CONSTITUTIVE RELATIONS

In this study we restrict ourself to bodies whose stored energy is such that

$$W := W(\mathbf{X}, J_1, J_2, J_3). \tag{8}$$

Then, the Cauchy stress is given by

$$\mathbf{T} = W_3\mathbf{1} + \frac{2}{J_3}[W_1\mathbf{B}_{\kappa R} - W_2\mathbf{B}_{\kappa R}^{-1}], \tag{9}$$

where, W_1, W_2, W_3 denote the derivatives of the stored energy function with respect to J_1, J_2, J_3, respectively. The stored energy W should be such that

$$W_3 \leq 0, \qquad W_1 > 0, \qquad W_2 \geq 0, \tag{10}$$

to satisfy E-inequalities (see Truesdell and Noll [1]). The Cauchy stress can be expressed as

$$\mathbf{T} = W_3\mathbf{1} + \mathbf{T}^c, \tag{11}$$

where $\mathbf{T}^c = \frac{2}{J_3}[W_1\mathbf{B}_{\kappa R} - W_2\mathbf{B}_{\kappa R}^{-1}]$. We find this decomposition convenient to present our results.

The homogeneous version of the stored energy function which we consider was proposed by Blatz and Ko [3]. The inhomogeneous form of this stored energy is given by

$$W = 0.5 * \mu_1(\mathbf{X})[\alpha(J_3) + \mu_2(\mathbf{X}) * (J_1 - 3) + (1 - \mu_2(\mathbf{X})) * (J_2 - 3)], \tag{12}$$

and the stress is obtained from (12) and (9) as

$$\mathbf{T} = \frac{\mu_1(\mathbf{X})}{J_3}[\mu_m(J_3)\mathbf{1} + \mu_2(\mathbf{X})\mathbf{B}_{\kappa R} - (1 - \mu_2(\mathbf{X}))\mathbf{B}_{\kappa R}^{-1}], \tag{13}$$

where $\alpha(J_3) = [\mu_2(\mathbf{X})(J_3^{-2\mu_3(\mathbf{X})} - 1) + (1 - \mu_2(\mathbf{X}))(J_3^{2\mu_3(\mathbf{X})} - 1)]/(\mu_3(\mathbf{X}))$, $\mu_m(J_3) = \frac{J_3}{2}\frac{d\alpha}{dJ_3} = [J_3^{2\mu_3(\mathbf{X})} - \mu_2(\mathbf{X})(J_3^{2\mu_3(\mathbf{X})} + J_3^{-2\mu_3(\mathbf{X})})]$. The parameter μ_3 is related to the Poisson ratio (ν) (see [3, 5]), $\mu_3 = \frac{\nu}{1-2\nu}$. It can be easily verified that the E-inequalities hold when $\mu_2(\mathbf{X}) = 1$ and $\mu_1(\mathbf{X}) > 0$. Horgan [23] showed that this corresponds to the case when the ellipticity condition is satisfied for all values of stretch. Wineman and Waldron [6] showed that when $\mu_2 = 1$, there exists a unique shear deformation corresponding to a given shear stress even in the absence of normal traction. We study in detail the case when $\mu_2 = 1$. Then, the stress is given by

$$\mathbf{T} = \frac{\mu_1(\mathbf{X})}{J_3}\left(-J_3^{-2\mu_3(\mathbf{X})}\mathbf{1} + \mathbf{B}_{\kappa R}\right). \tag{14}$$

We shall neglect body forces and as we shall consider only static problems, the balance of linear momentum reduces to

$$\operatorname{div}(\mathbf{T}) = \mathbf{0}. \tag{15}$$

Next we discuss the non-dimensionalization procedure. We first introduce a dimensionless prescription of the position, gradient and divergence through

$$\tilde{\mathbf{x}} = \frac{1}{L}\mathbf{x}, \quad \widetilde{\operatorname{grad}(\cdot)} = L * \operatorname{grad}(\cdot), \quad \widetilde{\operatorname{div}(\cdot)} = L * \operatorname{div}(\cdot), \tag{16}$$

where L is a relevant length scale, $\widetilde{\operatorname{grad}(\cdot)} = \frac{\partial(\cdot)}{\partial\tilde{\mathbf{x}}}$ and $\operatorname{grad}(\cdot) = \frac{\partial(\cdot)}{\partial\mathbf{x}}$. We note that the deformation gradient $\mathbf{F}_{\kappa R}$ is already a dimensionless quantity. We introduce a parameter, μ_o, with units of stress, to render the Cauchy stress dimensionless. The parameter μ_o depends on the specific form of the stored energy function. Here μ_o is assumed to be the mean value of μ_1. Thus, Equation (9) becomes

$$\tilde{\mathbf{T}} = \widetilde{W}_3\mathbf{1} + \frac{2}{J_3}\left[\widetilde{W}_1\mathbf{B}_{\kappa R} - \widetilde{W}_2\mathbf{B}_{\kappa R}^{-1}\right], \tag{17}$$

where, as usual, $\widetilde{W}_i = W_i/\mu_o$ and $\widetilde{\mathbf{T}} = \mathbf{T}/\mu_o$. Consequently, Equation (15) becomes

$$\widetilde{\mathrm{div}}(\widetilde{\mathbf{T}}) = \mathbf{0}. \tag{18}$$

For convenience we drop the tilde with the understanding that all the quantities considered henceforth are non-dimensional unless otherwise explicitly stated.

4. FORMS OF INHOMOGENEITIES

Here, we shall confine our investigations to a body $\mathcal{B}$ that is the annular region between two co-axial right circular cylinders:

$$\mathcal{B} = \{(R, \Theta, Z) | R_i \leq R \leq R_o, 0 \leq \Theta \leq 2\pi, 0 \leq Z \leq h\}, \tag{19}$$

and, in this study, we identify L, the characteristic length scale, with the outer radius, R_o.

Let $\gamma(\mathbf{X})$ denote any one of the material parameters $\mu_1(\mathbf{X})$ or $\mu_2(\mathbf{X})$ or $\mu_3(\mathbf{X})$. We assume that the material properties vary only along the radial direction, $\gamma(\mathbf{X}) = \gamma(R)$. Thus, μ_i are all functions of R. Before we discuss the manner in which the properties vary, we shall introduce a parameter $\overline{R}$ in terms of which we find it convenient to discuss the variation as this parameter ranges between 0 and 1:

$$\overline{R} = \frac{R - R_i}{R_o - R_i}. \tag{20}$$

The following functional forms for $\gamma(R)$ are such that

$$\gamma_{mean} = \frac{\int_{R_i}^{R_o} \gamma(R)\,\mathrm{d}R}{(R_o - R_i)} = \int_0^1 \gamma(\overline{R})\,\mathrm{d}\overline{R} = 1. \tag{21}$$

First, we shall consider cases where the material parameter varies monotonically. Here, we consider two types of variations, one in which $\gamma(\overline{R})$ increases from R_i to R_o and in the other in which it decreases. While this can happen in a variety of ways, we choose the following simple variations.

Linear variation:

$$\gamma(\overline{R}) = 2(1 - \delta)\overline{R} + \delta, \tag{22}$$

where $0 < \delta < 2$. Thus,

$$\frac{d\gamma}{d\overline{R}} \begin{cases} > 0, & 0 < \delta < 1, \\ < 0, & 1 < \delta < 2. \end{cases} \tag{23}$$

Exponential variation:

Here we suppose that

$$\gamma(\overline{R}) = \frac{\delta}{(e^{\delta} - 1)} * e^{\delta \overline{R}}, \tag{24}$$

where, $-\infty < \delta < \infty$. Thus,

$$\frac{d\gamma}{d\overline{R}} \begin{cases} > 0, & \delta > 0, \\ < 0, & \delta < 0. \end{cases} \tag{25}$$

We shall also study cases where the variation of μ is non-monotonic.

Piecewise constant (PWC) variation:

In this case we shall assume that

$$\gamma(\overline{R}) = \begin{cases} \delta + 2 * (1 - \delta) * \sum_{n=0}^{k-1} (-1)^n H(\overline{R} - \frac{n}{k}), & k \text{ is even}, \\ \delta + 2 * (1 - \delta) \frac{k}{(k+1)} \sum_{n=0}^{k-1} (-1)^n H(\overline{R} - \frac{n}{k}), & k \text{ is odd}, \end{cases} \tag{26}$$

$$\text{where} \quad H\left(\overline{R} - \frac{n}{k}\right) = \begin{cases} 0 & \text{if } \overline{R} < \frac{n}{k}, \\ 1 & \text{if } \overline{R} \geq \frac{n}{k}. \end{cases}$$

Here δ and k determine the amplitude and frequency of the variation.

Sinusoidal variation:

For such a variation, we assume that

$$\gamma(\overline{R}) = 1 + \delta * \sin(2k\pi\overline{R}), \tag{27}$$

where δ determines the amplitude of the variation and k the frequency.

Cosine variation:

Finally, we study the case

$$\gamma(\overline{R}) = 1 + \delta * \cos(2k\pi\overline{R}), \tag{28}$$

with the δ and k having the same meaning as in the previous case. We require that in all the above cases, k has to be an integer.

5. INFLATION, EXTENSION, TORSION AND SHEARING OF AN ANNULAR CYLINDER

We shall consider a reasonably large class of inhomogeneous deformations that have been studied in great detail for homogeneous isotropic elastic solids. We shall seek a semi-inverse solution of the following form, for the deformation, in cylindrical polar coordinates:

$$r = r(R), \qquad \theta = \phi(R) + \beta\Theta + \Omega Z, \qquad z = w(R) + \kappa\Theta + \lambda Z, \tag{29}$$

where (R,Θ,Z) and (r,θ,z) represent the coordinates of a typical material point, before and after deformation, respectively. In Equation (29), β, Ω, κ and λ are constants. The function $r(R)$ describes the inflation or deflation of the annular region, $\phi(R)$ denotes the circumferential shear of the annular region while $w(R)$ denotes the transverse or anti-plane shear. The constant Ω denotes the angle of twist per unit length of the undeformed cylinder, κ the azimuthal shear, λ the extension suffered by the body, and β is related to the angular displacements undergone by radial filaments.

As with all semi-inverse methods, the traction that is necessary to engender the deformation (29) can be calculated once the function and unknown parameters that appear in (29) are determined. The functions and unknown parameters are determined such that they satisfy the equilibrium equation (15) and the boundary conditions (yet to be specified). It is of course possible that these equations cannot be satisfied. But this is not to be construed as there being no other solutions to the BVP, for there could be solutions that have a different structure than the semi-inverse solution that is sought. Similarly, there can exist a multitude of other possible solutions that have a different structure that solve the BVP.

The deformation gradient $\mathbf{F}_{\kappa R}$ corresponding to the deformation (29) in a cylindrical coordinate system has the matrix representation given by

$$\mathbf{F}_{\kappa R} = \begin{pmatrix} r_{,R} & 0 & 0 \\ r\phi_{,R} & \beta\frac{r}{R} & r\Omega \\ w_{,R} & \frac{\kappa}{R} & \lambda \end{pmatrix}, \tag{30}$$

where $(.)_{,R}$ denotes $\frac{\mathrm{d}(.)}{\mathrm{d}R}$, a notation used throughout this paper. Then, the left stretch tensors $\mathbf{B}$ and $\mathbf{B}^{-1}$ have the following matrix representation:

$$\mathbf{B}_{\kappa R} = \begin{pmatrix} r_{,R}^2 & r\phi_{,R}\, r_{,R} & w_{,R}\, r_{,R} \\ r\phi_{,R}\, r_{,R} & (r\phi_{,R})^2 + (\beta\frac{r}{R})^2 + (r\Omega)^2 & r\Omega\lambda + r w_{,R}\,\phi_{,R} + \frac{r}{R^2}\beta\kappa \\ w_{,R}\, r_{,R} & r\Omega\lambda + r w_{,R}\,\phi_{,R} + \frac{r}{R^2}\beta\kappa & (\lambda)^2 + w_{,R}^2 + (\frac{\kappa}{R})^2 \end{pmatrix}, \tag{31}$$

$$\mathbf{B}^{-1}_{\kappa_R} = \begin{pmatrix} \frac{1}{r_{,R}^2}\{1+\frac{1}{\varphi^2}[(R\xi_1)^2+\xi_2^2]\} & \frac{1}{rr_{,R}\varphi^2}[\lambda\xi_1 R^2+\kappa\xi_2] & \frac{-1}{r_{,R}\varphi^2}[\Omega\xi_1 R^2+\beta\xi_2] \\ \frac{1}{rr_{,R}\varphi^2}[\lambda\xi_1 R^2+\kappa\xi_2] & \frac{1}{(r\varphi)^2}[\kappa^2+(R\lambda)^2] & \frac{-1}{r\varphi^2}[\beta\kappa+\Omega\lambda R^2] \\ \frac{-1}{r_{,R}\varphi^2}[\Omega\xi_1 R^2+\beta\xi_2] & \frac{-1}{r\varphi^2}[\beta\kappa+\Omega\lambda R^2] & \frac{1}{\varphi^2}[\beta^2+(R\Omega)^2] \end{pmatrix}, \tag{32}$$

where $\varphi = \beta\lambda - \Omega\kappa$, $\xi_1 = w_{,R}\Omega - \phi_{,R}\lambda$, $\xi_2 = w_{,R}\beta - \phi_{,R}\kappa$.

For this deformation

$$J_1 = r_{,R}^2 + (r\phi_{,R})^2 + (\beta\frac{r}{R})^2 + (r\Omega)^2 + (\lambda)^2 + w_{,R}^2 + \left(\frac{\kappa}{R}\right)^2, \tag{33}$$

$$J_2 = \frac{1}{r_{,R}^2}\left\{1+\frac{1}{\varphi^2}\left[(R\xi_1)^2+\xi_2^2\right]\right\} + \frac{1}{\varphi^2}\left\{\frac{\kappa^2+(R\lambda)^2}{r^2}+\beta^2+(R\Omega)^2\right\}, \tag{34}$$

$$J_3 = \frac{r}{R}r_{,R}\varphi. \tag{35}$$

It immediately follows that $r_{,R} > 0$. Also, if we do not allow inversion of the cylinder, $\varphi > 0$, hence $\beta\lambda > \Omega\kappa$, a restriction enforced in this study.

For the special form of the assumed deformation, the deformation gradient is only a function of R and therefore the stored energy has the form $W = W(\mathbf{F}_{\kappa_R}(R), R)$. Then the equilibrium equation (15) simplifies to

$$\frac{\mathrm{d}T_{rr}}{\mathrm{d}r} + \frac{1}{r}(T_{rr} - T_{\theta\theta}) = 0, \tag{36}$$

$$\frac{\mathrm{d}T_{r\theta}}{\mathrm{d}r} + \frac{2}{r}T_{r\theta} = 0, \tag{37}$$

$$\frac{\mathrm{d}T_{rz}}{\mathrm{d}r} + \frac{1}{r}T_{rz} = 0. \tag{38}$$

Equations (37) and (38) can be easily integrated to yield

$$T_{r\theta}(r) = \frac{r_i^2}{r^2}T_{r\theta}(r_i), \tag{39}$$

$$T_{rz}(r) = \frac{r_i}{r}T_{rz}(r_i). \tag{40}$$

Here, the stresses at the inner surface are assumed to be known. Substituting for $T_{r\theta}(r)$ and $T_{rz}(r)$ in (39) and (40), we get two equations in terms of $(r_{,R}, \phi_{,R}, w_{,R})$. Thus, treating these derivatives as variables, Equations (39), (40) are solved simultaneously for $\phi_{,R}$ and $w_{,R}$ in terms of $r_{,R}$. Then, $r_{,R}$ is obtained by solving the second-order ordinary differential equation of the form

$$f_1(r, R, r_{,R})r_{,RR} + f_2(r, R, r_{,R}) = 0, \tag{41}$$

obtained from (36) by substituting the solutions obtained for $\phi_{,R}$ and $w_{,R}$, along with the mixed boundary condition[1]

$$r(R_i) = r_i, \qquad T_{rr}(r_o) = P_o. \tag{42}$$

Equation (41) along with the boundary condition (42) is solved numerically. Ensuring that $f_1(r, R, r_{,R}) \neq 0$, we begin by solving the initial-value problem (IVP)

$$r_{,RR} = \frac{-f_2}{f_1}, \qquad r(R_i) = r_i, \qquad r_{,R}(R_i) = r_R^i, \tag{43}$$

for some particular value of r_R^i. Then, we evaluate the boundary condition $T_{rr}(r(R_o))$. Unless it happens that the value for this equals P_o, we take a different value for r_R^i and solve the resulting IVP. Thus, the error

$$e(r_R^i) \equiv P_o - P_o^{comp}(r_R^i) = 0, \tag{44}$$

where P_o^{comp} is the value of T_{rr} computed at $R = R_o = 1$, is a function of our choice for the initial slope. Now, the problem is to solve the non-linear equation (44) for r_R^i. This non-linear equation is solved using the bisection technique in which zero is approximated to be 10^{-9}.

The IVP (43) can be solved using a variety of techniques, each with its attendant advantages and disadvantages. Here, we convert the second-order ODE to a system of two first-order ODEs by a simple change of variables:

$$u = r, \qquad v = r_{,R}. \tag{45}$$

The differential equations relating these functions are

$$u_{,R} = v, \qquad v_{,R} = \frac{-f_2}{f_1} = g(R, u, v), \tag{46}$$

with the initial condition

$$u(R_i) = r_i, \qquad v(R_i) = r_R^i. \tag{47}$$

This system of first-order ODEs is integrated numerically using ODE45 in Matlab.

5.1. Solution Scheme for Piecewise Constant Variation

For this case, the variation of the material parameter is discontinuous. Hence, the governing equation (41) has to be solved in each sub-domain where the parameter varies continuously and at the interface we require $\mathbf{t_n} = -\mathbf{t}_{-\mathbf{n}}$, where $\mathbf{n}$ ($= \mathbf{e}_r$, for the assumed form of deformation and inhomogeneity) is the normal to the interface and the deformation field is assumed to be continuous at the interface. Here, in other words, we assume that there is no

de-bonding at the interface. This translates into requiring T_{rr}, $T_{r\theta}$ and T_{rz} apart from r to be continuous across the interface. Equations (39) and (40) ensure the continuity of $T_{r\theta}$ and T_{rz} respectively. However, the continuity of T_{rr} has to be enforced. Towards this purpose, let $R_1, R_2, \ldots, R_n$ denote the locations where the material parameter is discontinuous. We begin by solving the IVP

$$r_{,RR} = \frac{-f_2}{f_1}, \qquad r(R_i) = r_i, \qquad r_{,R}(R_i) = r_R^i, \tag{48}$$

over the domain $R_i \leq R < R_1$, guessing a value for r_R^i. Now, the values of $r(R_1^-) = r_1^-$ and $r_{,R}(R_1^-) = r_{R_1}^-$ are known. Then, the value of $r_{,R}(R_1^+) = r_{R_1}^+$ is obtained by solving the equation

$$T_{rr}(r_1^+, R_1^+, r_{R_1}^+) = T_{rr}(r_1^-, R_1^-, r_{R_1}^-), \tag{49}$$

which is non-linear, in general, using the bisection algorithm. Note here that $r_1^+ = r_1^-$, and the only unknown is $r_{R_1}^+$. Having obtained $r_{R_1}^+$, we solve the IVP

$$r_{,RR} = \frac{-f_2}{f_1}, \qquad r(R_1^+) = r_1^+, \qquad r_{,R}(R_1^+) = r_{R_1}^+, \tag{50}$$

over the domain $R_1 < R < R_2$. This process is continued until the boundary of the body (i.e. $R = R_o$) is reached. Now, from the values of $r(R_o)$ and $r_{,R}(R_o)$, P_o^{comp} and the error e are computed. Unless the computed error is within the tolerance, we iterate guessing a new value for r_R^i, using the same iterative scheme outlined above.

To be able to discuss solutions to a specific BVP, we have to decide what the appropriate boundary conditions are. For instance, we could ask if a deformation such as that being considered is possible, given say a purely radial stress applied at the inner radius of an annular cylinder. Then, we could compute the traction that ought to be applied at the outer surface to acheive the sought deformation. Before discussing specific BVPs, we shall document the forms that the equilibrium equation takes for the specific stored energy that we discussed earlier.

5.2. Solution Using the Blatz–Ko Form of the Stored Energy Function

When $\mathbf{T}$ is given by (13), Equations (39) and (40) simplify to

$$a_1\phi_{,R} + a_2 w_{,R} = a_3, \tag{51}$$

$$b_1\phi_{,R} + b_2 w_{,R} = b_3, \tag{52}$$

where

$$a_1 = \mu_1^* r r_{,R} + \mu_2^* \frac{(R\lambda)^2 + \kappa^2}{r r_{,R} \varphi^2}, \; a_2 = -\mu_2^* \frac{\Omega\lambda R^2 + \kappa\beta}{r r_{,R} \varphi^2}, \; a_3 = \frac{c_1 r_{,R} \varphi}{Rr}, \tag{53}$$

$$b_1 = ra_2, b_2 = \mu_1^* r_{,R} + \mu_2^* \frac{(R\Omega)^2 + \beta^2}{r_{,R}\varphi^2}, b_3 = \frac{c_2 r_{,R}\varphi}{R}, \tag{54}$$

with $c_1 = r_i^2 T_{r\theta}(r_i)$ and $c_2 = r_i T_{rz}(r_i)$, $\mu_1^* = \mu_1(R) * \mu_2(R)$, $\mu_2^* = \mu_1(R) * (1 - \mu_2(R))$. A straightforward algebraic simplification yields

$$g_1 = a_1 b_2 - a_2 b_1 = \mu_1^{*2} r r_{,R}^2 + \mu_1^* \mu_2^* * d_1 + \mu_2^{*2} * e_1 \tag{55}$$

where $d_1 = \frac{(R\lambda)^2 + \kappa^2 + r^2(\beta^2 + (R\Omega)^2)}{r\varphi^2} > 0$, $e_1 = \frac{(R)^2}{r(\varphi r_{,R})^2} > 0$. Now, we are interested in finding if $g_1 = 0$. At a given location R (say R_a), we can determine the value(s) of $\frac{\mu_2^*}{\mu_1^*}$ when this can happen by evaluating

$$\frac{\mu_2^*}{\mu_1^*} = \frac{-d_1^2 \pm \sqrt{d_1^4 - 4 r r_{,R}^2 e_1}}{2e_1^2}. \tag{56}$$

It can be easily verified that $\frac{\mu_2^*}{\mu_1^*} < 0$. If $\mu_1(R) > 0$ and $0 \le \mu_2(R) \le 1$, then $\frac{\mu_2^*}{\mu_1^*} > 0$, resulting in $a_1 b_2 - a_2 b_1 \neq 0$. Since, in this study we assume $\mu_1(R) > 0$ and $0 \le \mu_2(R) \le 1$, there exists a solution for the system of Equations (51) and (52), solving which we obtain

$$\phi_{,R} = \frac{g_2}{g_1}, w_{,R} = \frac{g_3}{g_1}, \tag{57}$$

where

$$g_2 = b_2 a_3 - a_2 b_3 = c_1 \varphi \mu_1^* \frac{r_{,R}^2}{Rr} + \frac{\mu_2^*}{Rr\varphi} d_2, \tag{58}$$

$$g_3 = b_3 a_1 - a_3 b_1 = c_2 \varphi \mu_1^* \frac{r r_{,R}^2}{R} + \frac{\mu_2^*}{Rr\varphi} d_3, \tag{59}$$

with $d_2 = c_1[(R\Omega)^2 + \beta^2] + c_2[\Omega\lambda R^2 + \kappa\beta]$, $d_3 = c_2[(R\lambda)^2 + \kappa^2] + c_1[\Omega\lambda R^2 + \kappa\beta]$.

Next, we need to find $\phi_{,RR}$ and $w_{,RR}$. Towards this end we note that

$$d_{1,R} = \frac{r_{,R}}{\varphi^2}\left[\beta^2 + (R\Omega)^2 - \frac{\kappa^2 + (R\lambda)^2}{r^2}\right] + 2\frac{R}{\varphi^2}\left[\frac{\lambda^2}{r} + r\Omega^2\right], \tag{60}$$

$$m_1 = \mu_{1,R}^* (2\mu_1^* r r_{,R}^2 + \mu_2^* d_1) + \mu_{2,R}^* \left(\mu_1^* d_1 + \frac{2\mu_2^* R^2}{r(r_{,R}\varphi)^2}\right), \tag{61}$$

$$h_1 = \mu_1^{*2} r_{,R}^3 + \frac{\mu_2^{*2} R}{r\varphi^2 r_{,R}^2}\left(2 - \frac{R}{r}\right) + \mu_1^* \mu_2^* d_{1,R}, \tag{62}$$

$$n_1 = \mu_1^{*2} r r_{,R} - \frac{(\mu_2^* R)^2}{r r_{,R}^3 \varphi^2}, \tag{63}$$

$$g_{1,R} = 2n_1 r_{,RR} + m_1 + h_1, \tag{64}$$

$$d_{2,R} = 2R\Omega[c_1\Omega + c_2\lambda], \tag{65}$$

$$m_2 = \mu^*_{1,R}\, c_1\varphi\frac{r^2_{,R}}{Rr} + \frac{\mu^*_{2,R}}{Rr\varphi}d_2, \tag{66}$$

$$h_2 = \frac{\mu^*_2}{rR\varphi}d_{2,R} - \frac{r + Rr_{,R}}{(Rr)^2}\left[c_1\varphi\mu^*_1 r^2_{,R} + \mu^*_2\frac{d_2}{\varphi}\right], \tag{67}$$

$$n_2 = c_1\varphi\frac{\mu^*_1 r_{,R}}{Rr}, \tag{68}$$

$$g_{2,R} = 2n_2 r_{,RR} + m_2 + h_2, \tag{69}$$

$$\phi_{,RR} = 2\left(\frac{n_2}{g_1} - \frac{n_1 g_2}{g_1^2}\right)r_{,RR} + \frac{m_2 + h_2}{g_1} - \frac{g_2}{g_1^2}(m_1 + h_1), \tag{70}$$

$$d_{3,R} = 2R\lambda[c_1\Omega + c_2\lambda], \tag{71}$$

$$m_3 = \mu^*_{1,R}\, c_2\varphi\frac{rr^2_{,R}}{R} + \mu^*_{2,R}\frac{d_3}{Rr\varphi}, \tag{72}$$

$$h_3 = c_2\varphi\mu^*_1\left[\frac{r_{,R}}{R} - \frac{r}{R^2}\right] + \frac{\mu^*_2}{Rr\varphi}d_{3,R} - \frac{\mu^*_2 d_3}{\varphi(Rr)^2}[r_{,R}R + r], \tag{73}$$

$$n_3 = c_2\varphi\frac{\mu^*_1 r}{R}r_{,R}, \tag{74}$$

$$g_{3,R} = 2n_3 r_{,RR} + m_3 + h_3, \tag{75}$$

$$w_{,RR} = 2\left(\frac{n_3}{g_1} - \frac{n_1 g_3}{g_1^2}\right)r_{,RR} + \frac{m_3 + h_3}{g_1} - \frac{g_3}{g_1^2}(m_1 + h_1), \tag{76}$$

The radial component of the balance of linear momentum (36) can be written as

$$\frac{\mathrm{d}T_{rr}}{\mathrm{d}R} + \frac{r_{,R}}{r}(T_{rr} - T_{\theta\theta}) = 0. \tag{77}$$

To compute $\dfrac{\mathrm{d}T_{rr}}{\mathrm{d}R}$ we start by defining

$$x_1 = 2\left[\left(\frac{n_3}{g_1} - \frac{g_3 n_1}{g_1^2}\right)\Omega - \lambda\left(\frac{n_2}{g_1 - \frac{g_2 n_1}{g_1^2}}\right)\right], \tag{78}$$

$$x_2 = 2\left[\left(\frac{n_3}{g_1} - \frac{g_3 n_1}{g_1^2}\right)\beta - \kappa\left(\frac{n_2}{g_1 - \frac{g_2 n_1}{g_1^2}}\right)\right], \tag{79}$$

$$y_1 = \frac{1}{g_1}[(m_3 + h_3)\Omega - \lambda(m_2 + h_2)] - \frac{(m_1 + h_1)}{g_1^2}(g_3\Omega - \lambda g_2), \tag{80}$$

$$y_2 = \frac{1}{g_1}[(m_3 + h_3)\beta - \kappa(m_2 + h_2)] - \frac{(m_1 + h_1)}{g_1^2}(g_3\beta - \kappa g_2), \tag{81}$$

Then, we immediately obtain

$$\xi_{1,R} = x_1 r_{,RR} + y_1, \tag{82}$$

$$\xi_{2,R} = x_2 r_{,RR} + y_2, \tag{83}$$

and hence it follows that

$$B^{-1}_{rr,R} = \frac{2}{r_{,R}} \left\{ \frac{(R^2 \xi_1 x_1 + \xi_2 x_2)}{r_{,R}} - B^{-1}_{rr} \right\} r_{,RR} + \frac{2}{r^2_{,R}} [R(\xi_1^2 + R\xi_1 y_1) + \xi_2 y_2], \tag{84}$$

Noting that

$$J_{3,R} = \frac{\varphi}{R} \left(r^2_{,R} + r r_{,RR} - \frac{r r_{,R}}{R} \right), \tag{85}$$

$$\frac{\mathrm{d}\mu_m}{\mathrm{d}J_3} = \frac{2\mu_3}{J_3} \left[J_3^{2\mu_3} - \mu_2 (J_3^{2\mu_3} - J_3^{-2\mu_3}) \right] \tag{86}$$

and defining

$$m_{\mu_m} = \mu_{1,R} \mu_m + \mu_1 \{ 2\mu_{3,R} \ln(J_3) [J_3^{2\mu_3} - \mu_2 (J_3^{2\mu_3} - J_3^{-2\mu_3})] - \mu_{2,R} (J_3^{2\mu_3} + J_3^{-2\mu_3}) \}, \tag{87}$$

$$m_4 = m_{\mu_m} + (\mu_{1,R} \mu_2 + \mu_1 \mu_{2,R}) B_{rr} - (\mu_{1,R} (1 - \mu_2) - \mu_1 \mu_{2,R}) B^{-1}_{rr}, \tag{88}$$

we compute

$$T_{rr,R} = \frac{1}{J_3} \left\{ m_4 + \left[\mu_1 \frac{\mathrm{d}\mu_m}{\mathrm{d}J_3} - T_{rr} \right] J_{3,R} + 2\mu_1 \mu_2 r_{,R} r_{,RR} - \mu_1 (1 - \mu_2) B^{-1}_{rr,R} \right\}. \tag{89}$$

Consequently, Equation (77) simplifies to

$$\frac{f_1}{J_3} r_{,RR} + \frac{f_2}{J_3} = 0, \tag{90}$$

where

$$f_1 = \varphi \left(\mu_1 \frac{\mathrm{d}\mu_m}{\mathrm{d}J_3} - T_{rr} \right) \frac{r}{R} + 2\mu_1 \left\{ \mu_2 r_{,R} + \frac{(1 - \mu_2)}{r_{,R}} \left[B^{-1}_{rr} - \frac{1}{r_{,R}} (R^2 \xi_1 x_1 + \xi_2 x_2) \right] \right\}, \tag{91}$$

$$l_2 = m_4 + \left(\mu_1 \frac{\mathrm{d}\mu_m}{\mathrm{d}J_3} - T_{rr} \right) \left(r_{,R} - \frac{r}{R} \right) \frac{r_{,R} \varphi}{R}$$

$$-2\frac{\mu_1(1-\mu_2)}{r_{,R}^2}[R(\xi_1^2+R\xi_1 y_1)+\xi_2 y_2], \tag{92}$$

$$l_1 = \mu_1\frac{r_{,R}}{r}\left[\mu_2(B_{rr}-B_{\theta\theta})-(1-\mu_2)(B_{rr}^{-1}-B_{\theta\theta}^{-1})\right], \tag{93}$$

$$f_2 = l_1+l_2. \tag{94}$$

We can immediately simplify (90) to the form

$$f_1(r,R,r_{,R})r_{,RR}+f_2(r,R,r_{,R})=0, \tag{95}$$

which, as expected, has the same form as (41).

Before proceeding further, we record the forms of f_1 and f_2 for a few special cases. First, if $\mu_2(R)=1$, then

$$f_1 = \varphi\left(2\mu_1\mu_3 J_3^{-(2\mu_3+1)}-T_{rr}\right)\frac{r}{R}+2\mu_1 r_{,R}, \tag{96}$$

$$f_2 = \mu_1(B_{rr}-B_{\theta\theta})\frac{r_{,R}}{r}+(2\mu_1\mu_3 J_3^{-(2\mu_3+1)}-T_{rr})\left(r_{,R}-\frac{r}{R}\right)\frac{r_{,R}\varphi}{R}$$
$$+\mu_{1,R}(-J_3^{-2\mu_3}+B_{rr})+2\mu_1\ln(J_3)\mu_{3,R}J_3^{-2\mu_3}. \tag{97}$$

Since we would like to consider inflation, extension and torsion of an annular or solid cylinder, $\beta=1$, $\kappa=T_{rz}(r_i)=0$ and $T_{r\theta}(r_i)=0$. Consequently, $\phi(R)=0$, $w(R)=0$. For this case

$$f_1 = \varphi\left(\mu_1\frac{\mathrm{d}\mu_m}{\mathrm{d}J_3}-T_{rr}\right)\frac{r}{R}+2\mu_1\left[\mu_2 r_{,R}+\frac{(1-\mu_2)}{r_{,R}^3}\right], \tag{98}$$

$$l_2 = m_4+\left(\mu_1\frac{\mathrm{d}\mu_m}{\mathrm{d}J_3}-T_{rr}\right)\left(r_{,R}-\frac{r}{R}\right)\frac{r_{,R}\varphi}{R},$$

$$l_1 = \mu_1\frac{r_{,R}}{r}\left\{\mu_2\left[r_{,R}^2-\left(\frac{r}{R}\right)^2-(r\Omega)^2\right]-(1-\mu_2)\left[\frac{1}{r_{,R}^2}-\left(\frac{R}{r}\right)^2\right]\right\},$$

$$T_{rr} = \frac{\mu_1}{J_3}\left[\mu_m+\mu_2 r_{,R}^2-(1-\mu_2)\frac{1}{r_{,R}^2}\right]. \tag{99}$$

We note that numerical computation of the above is not possible at $R=0$. Hence, we compute the above quantities analytically and use them in the numerical scheme. Towards this end we find the following limits useful:

$$\lim_{R\to 0}\frac{r(R)}{R} = r_{,R}(0)\neq 0, \tag{100}$$

$$\lim_{R\to 0}\frac{Rr_{,R}-r}{R^2} = 0.5r_{,RR}(0), \tag{101}$$

$$\lim_{R\to 0}\frac{r^2-(r_{,R}R)^2}{r^3r_{,R}^2} = -\frac{r_{,RR}(0)}{r_{,R}^4(0)}, \tag{102}$$

$$\lim_{R\to 0}\frac{(r_{,R}R)^2-r^2}{rR^2} = r_{,RR}(0). \tag{103}$$

It then immediately follows that

$$J_3 = \lambda r_{,R}^2(0), \tag{104}$$

$$l_1 = \mu_1(0)\left[\mu_2(0)+(1-\mu_2(0))\frac{1}{r_{,R}^4(0)}\right]r_{,R}(0)r_{,RR}(0), \tag{105}$$

$$l_2 = m_4(0)+0.5\lambda\left[\mu_1(0)\frac{\mathrm{d}\mu_m}{\mathrm{d}J_3}(0)-T_{rr}(R=0)\right]r_{,R}(0)r_{,RR}(0), \tag{106}$$

$$f_1 = \lambda(\mu_1(0)\frac{\mathrm{d}\mu_m}{\mathrm{d}J_3}(0)-T_{rr}(R=0))r_{,R}(0) + 2\mu_1(0)\left[\mu_2(0)r_{,R}(0)+\frac{(1-\mu_2(0))}{r_{,R}(0)^3}\right]. \tag{107}$$

Hence, Equation (41) at $R=0$ takes the form

$$-m_4(0) = 3\left\{\mu_1(0)\left[\mu_2(0)+(1-\mu_2(0))\frac{1}{r_{,R}^4(0)}\right] + 0.5\lambda\left[\mu_1(0)\frac{\mathrm{d}\mu_m}{\mathrm{d}J_3}(0)-T_{rr}(R=0)\right]\right\}r_{,R}(0)r_{,RR}(0). \tag{108}$$

Hence, at $R=0$, the above expression is used to obtain $r_{,RR}(0)$. If the material parameters are constant, then $m_4=0$. In that case for (108) to hold for any arbitrary choice of[2] $r_{,R}(0)$ and/or λ, $r_{,RR}(0)=0$.

Before, proceeding further we note that we were unable to show a priori that $f_1\neq 0$. However, when this condition was checked numerically, for all the cases considered here $f_1\neq 0$.

6. GLOBAL QUANTIFIERS

In this and the following section, we provide more evidence to support the thesis of Saravanan and Rajagopal [20] that great care has to be exercised in approximating inhomogeneous bodies as homogeneous bodies, however mild their inhomogeneities. Let us consider the

inflation and axial extension, and torsion of an annular or solid right circular cylinder. Thus, $\beta = 1, \kappa = \phi = w = 0$. Suppose , we consider the Blatz–Ko model with $\mu_2 = 1$. In this case the stored energy is a function of only the first and third invariants of C. For this case, we obtain the following expressions.

The axial load, $\mathcal{L}$ defined through

$$\mathcal{L} = 2\pi \int_{r_i}^{r_o} T_{zz}\, r\, \mathrm{d}r, \tag{109}$$

simplifies to

$$\mathcal{L} = \pi \int_{r_i}^{r_o} (2 * T^e_{zz} - T^e_{rr} - T^e_{\theta\theta}) r\, \mathrm{d}r + \pi(r_o^2 * T_{rr}(r_o) - r_i^2 * T_{rr}(r_i)), \tag{110}$$

when the stresses are a function of only r. For the present case (110) reduces to

$$\mathcal{L} - L_p = \frac{2\pi}{\lambda} \int_{R_i}^{R_o} W_1 \left(2\lambda^2 - r_{,R}^2 - \left(\frac{r}{R}\right)^2 - (r\Omega)^2\right) R\, \mathrm{d}R, \tag{111}$$

where $L_p = \pi(r_o^2 * T_{rr}(r_o) - r_i^2 * T_{rr}(r_i))$.

Next, the expression for torque, $\mathcal{T}$ is given by

$$\mathcal{T} = 2\pi \int_{r_i}^{r_o} T_{\theta z}\, r^2\, \mathrm{d}r, \tag{112}$$

which in the present case reduces to

$$\mathcal{T} = 4\pi\Omega \int_{R_i}^{R_o} W_1 R r^2\, \mathrm{d}R. \tag{113}$$

The moment

$$\mathcal{M} = \int_0^h \int_{r_i}^{r_o} T_{\theta\theta} r\, \mathrm{d}r\, \mathrm{d}z \tag{114}$$

reduces to

$$\mathcal{M} = \frac{1}{2}\left[(r_o^2 T_{rr}(r_o) - r_i^2 T_{rr}(r_i)) + \int_{r_i}^{r_o} (T^e_{rr} - T^e_{\theta\theta}) r\, \mathrm{d}r\right], \tag{115}$$

per unit length of the cylinder in the current configuration, when the stress is a function of r only. In the present case it can be written as

$$\mathcal{M} - M_p = \frac{1}{\lambda} \int_{R_i}^{R_o} W_1 \left[r_{,R}^2 - \left(\frac{r}{R}\right)^2 - (r\Omega)^2\right] R\, \mathrm{d}R, \tag{116}$$

where $M_p = 0.5 * (r_o^2 * T_{rr}(r_o) - r_i^2 * T_{rr}(r_i))$.

Finally, even though this is not a global quantity, the radial component of normal stress at r_i is an often inferred experimental quantity, and this stress, which we denote by $\mathcal{P}$, is given by

$$\mathcal{P} = -T_{rr}(r_i) = -T_{rr}(r_o) - \int_{r_i}^{r_o} (T^e_{rr} - T^e_{\theta\theta})\frac{\mathrm{d}r}{r}, \tag{117}$$

which reduces to

$$\mathcal{P} = -T_{rr}(r_o) + \frac{2}{\lambda}\int_{R_i}^{R_o} W_1 \left[\left(\frac{r}{R}\right)^2 + (r\Omega)^2 - r_{,R}^2\right]\frac{R}{r^2}\,\mathrm{d}R. \tag{118}$$

Of course, we could obtain $\mathcal{P}$ directly as $-T_{rr}(r_i)$.

Having obtained these general expressions we now illustrate the role of the inhomogeneity within the context of the special stored energy functions introduced in Section 3 and the various forms of inhomogeneities introduced in Section 4. First we study the special form of the Blatz–Ko stored energy function (14). Let $(\mu_1)_{exp}$ denote the constant value of the material parameter μ_1 for the homogenized approximation for the inhomogeneous body of the same type. Then, we determine the value of $(\mu_1)_{exp}$ through a correlation with the experiment, such that both the homogeneous and inhomogeneous body require the same boundary traction to engender a given stretch or inflation. We propose to correlate with various experiments to obtain $(\mu_1)_{exp}$ and compare their values. Towards this purpose we begin by considering the classical uniaxial extension experiment.

6.1. Case 1: Uniaxial Extension

Here we consider the uniaxial extension of an annular or solid right circular cylinder, i.e. $\Omega = T_{rr}(r_i) = T_{rr}(r_o) = 0$. For this case, (111) reduces to

$$\begin{aligned}
\frac{\lambda\mathcal{L}(\lambda)}{2\pi} &= \int_{R_i}^{R_o} \mu_1(R)\left[2\lambda^2 - r_{,R}^2 - \left(\frac{r}{R}\right)^2\right] R\,\mathrm{d}R \\
&= (\mu_1)_{exp}\left[\lambda^2 - \lambda^{-\frac{2(\mu_3)^{Ax-Ext}_{exp}}{(2(\mu_3)^{Ax-Ext}_{exp}+1)}}\right](R_o^2 - R_i^2), \\
(\mu_1)^{Ax-Ext}_{exp} &= \frac{\int_{R_i}^{R_o} \mu_1(R)[2\lambda^2 - r_{,R}^2 - (\frac{r}{R})^2]R\,\mathrm{d}R}{\left[\lambda^2 - \lambda^{-\frac{2(\mu_3)^{Ax-Ext}_{exp}}{(2(\mu_3)^{Ax-Ext}_{exp}+1)}}\right](R_o^2 - R_i^2)}.
\end{aligned} \tag{119}$$

Before proceeding further a few comments are in order. While the homogeneous cylinder for this case permits a homogeneous deformation, the inhomogeneous cylinder, in general does not. However, when μ_3 is constant the deformation is homogeneous. This is consistent with the observation of Saravanan [24] who found necessary conditions for an inhomogeneous body to sustain homogeneous deformations. The value of $(\mu_1)^{Ax-Ext}_{exp}$ depends

on how $\mu_1(R)$ and $\mu_3(R)$ vary about the same mean and also on the value of $(\mu_3)_{exp}^{Ax-Ext}$ and λ. This clearly indicates that the inhomogeneous Blatz–Ko body in general cannot be approximated by a homogeneous Blatz–Ko body. However, if μ_3 is constant such an approximation is possible, for this BVP. Figure 1 plots the variation of $(\mu_1)_{exp}^{Ax-Ext}$ with R_i when μ_3 is assumed to be constant and $\mu_1(R)$ varies linearly and is piecewise constant, respectively. Thus, depending on the geometry of the body we could conclude the value for $(\mu_1)_{exp}^{Ax-Ext}$ varies by as much as 40 %. We note that for this case $(\mu_1)_{exp}^{Ax-Ext}$ does not vary with λ. Figure 2 depicts the variation of $(\mu_1)_{exp}^{Ax-Ext}$ with λ when $\mu_1(R)$ is constant and $\mu_3(R)$ varies exponentially and as a piecewise constant. For this case, we assume $(\mu_3)_{exp}^{Ax-Ext} = \mu_3^{mean} = 0.5$ (equivalently a mean Poisson ratio of 0.25 and varying from 0.33 to 0.15).

6.2, Case 2: Pure Twist

Next we consider the twisting of an annular or solid cylinder. A suitable axial load and $T_{rr}(r_i)$ is applied such that $r_i = R_i, \lambda = 1$. Also, $T_{rr}(r_o) = 0$. Then, we correlate the torque required to engender a given twist (Ω), to obtain

$$\frac{\mathcal{T}(\Omega)}{4\pi\Omega} = \int_{R_i}^{R_o} \mu_1(R) R r^2 \, dR = (\mu_1)_{exp} \int_{R_i}^{R_o} R r^{*2} \, dR,$$

$$(\mu_1)_{exp}^{Tr-Twt} = \frac{\int_{R_i}^{R_o} \mu_1(R) R r^2 \, dR}{\int_{R_i}^{R_o} R r^{*2} \, dR}, \tag{120}$$

from (113). It should be recognized that the $r(R)$ obtained for the inhomogeneous cylinder will be different from that obtained for the homogeneous cylinder ($r^*(R)$) and will depend on the parameters μ_3 and Ω.

For the same experiment, instead of correlating the torque required to engender a given twist, we can correlate the radial component of the normal stress required to ensure $r_i = R_i$ for a given twist to yield

$$0.5\mathcal{P} = \int_{R_i}^{R_o} \mu_1(R) \left[\left(\frac{r}{R} \right)^2 + (r\Omega)^2 - r_{,R}^2 \right] \frac{R}{r^2} \, dR$$

$$= (\mu_1)_{exp} \int_{R_i}^{R_o} \left[\left(\frac{r^*}{R} \right)^2 + (r^*\Omega)^2 - r_{,R}^{*2} \right] \frac{R}{r^{*2}} \, dR$$

$$(\mu_1)_{exp}^{Pr-Twt} = \frac{\int_{R_i}^{R_o} \mu_1(R) [(\frac{r}{R})^2 + (r\Omega)^2 - r_{,R}^2] \frac{R}{r^2} \, dR}{\int_{R_i}^{R_o} [(\frac{r^*}{R})^2 + (r^*\Omega)^2 - r_{,R}^{*2}] \frac{R}{r^{*2}} \, dR} \tag{121}$$

from (118). Similarly, we can correlate the axial load required to maintain $\lambda = 1$, for a given twist (Ω). Then

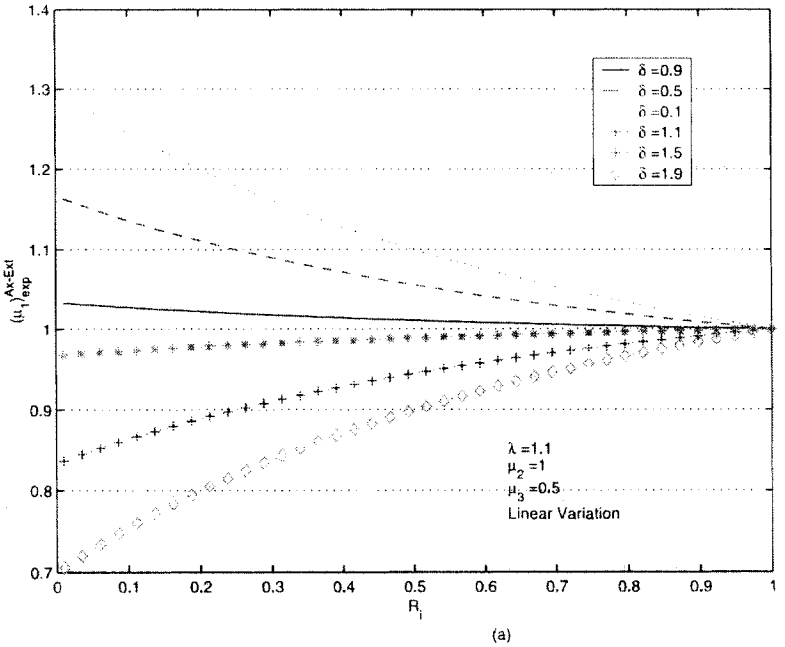

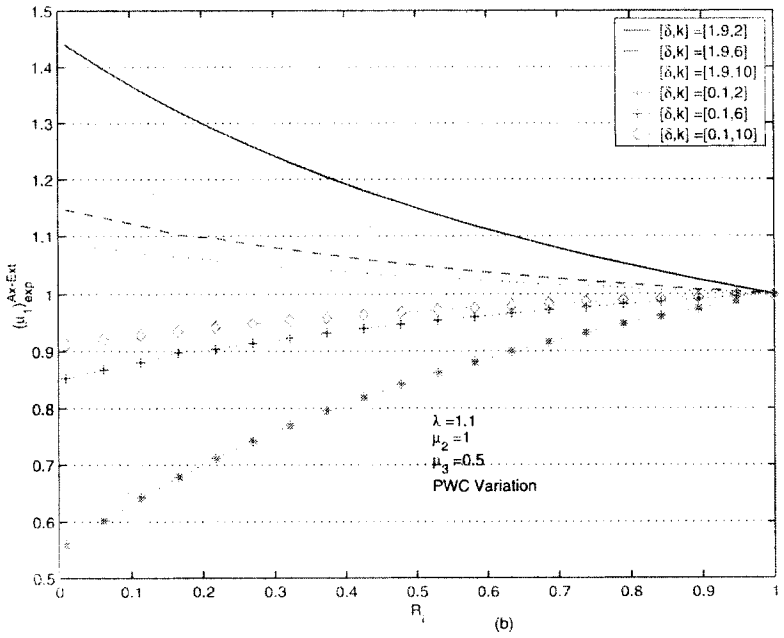

Figure 1. Plot of $(\mu_1)_{exp}^{Ax-Ext}$ vs R_i when μ_2, μ_3 are constant and $\mu_1(\overline{R}) =$ (a) $2(1-\delta)\overline{R}+\delta$, (b) $\sum_{n=0}^{k-1}(-1)^n H(\overline{R}-\frac{n}{k})$.

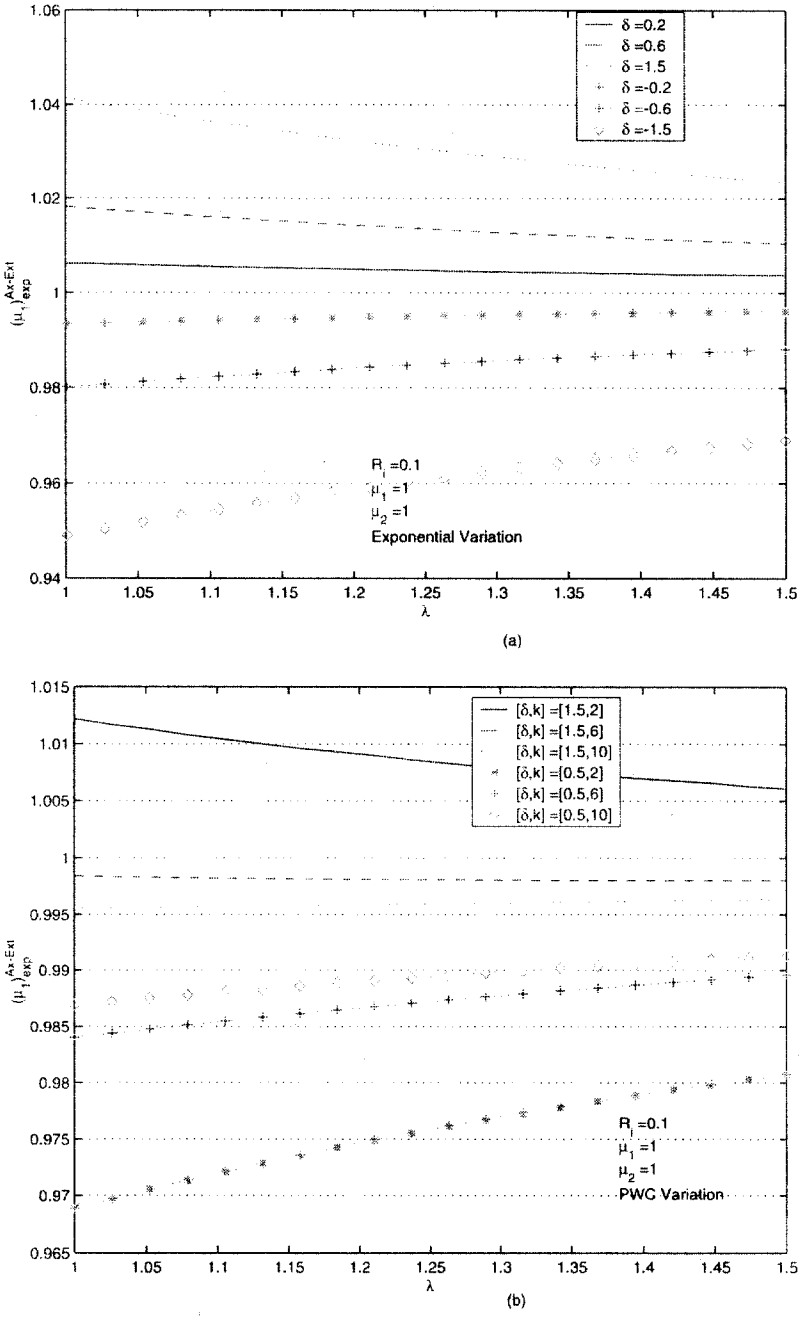

Figure 2. Plot of $(\mu_1)_{exp}^{Ax-Ext}$ vs λ when μ_1, μ_2 are constant and $\mu_3(\overline{R})$ = (a) $2(1-\delta)\overline{R}+\delta$, (b) $\sum_{n=0}^{k-1}(-1)^n H(\overline{R}-\frac{n}{k})$.

$$\begin{aligned}
\frac{(\mathcal{L}(\Omega) - L_p(\Omega))}{2\pi} &= \int_{R_i}^{R_o} \mu_1(R) \left[2 - r_{,R}^2 - \left(\frac{r}{R}\right)^2 - (r\Omega)^2\right] R\,\mathrm{d}R, \\
&= (\mu_1)_{exp} \int_{R_i}^{R_o} \left[2 - r_{,R}^{*2} - \left(\frac{r^*}{R}\right)^2 - (r^*\Omega)^2\right] R\,\mathrm{d}R, \\
(\mu_1)_{exp}^{Ax-Twt} &= \frac{\int_{R_i}^{R_o} \mu_1(R) \left[2 - r_{,R}^2 - (\frac{r}{R})^2 - (r\Omega)^2\right] R\,\mathrm{d}R}{\int_{R_i}^{R_o} \left[2 - r_{,R}^{*2} - (\frac{r^*}{R})^2 - (r^*\Omega)^2\right] R\,\mathrm{d}R} \qquad (122)
\end{aligned}$$

from (111). Here we have assumed the correlation of $T_{rr}(r_i)$ to ensure L_p to be same for both the homogeneous and inhomogeneous body. We emphasize again that both the inhomogeneous body and its homogeneous counterpart are subjected to the same boundary deformation and we are examining the appropriateness of the approximation by comparing the experimentally measurable quantities, like the axial load, torque, etc., required to maintain the prescribed boundary deformation.

Figures 3 and 4 capture the variation of $(\mu_1)_{exp}$ with Ω for various variations of $\mu_1(R)$ about a mean value of 1. In these figures $\mu_3 = 0.5$, a constant. The results clearly suggest that, for at least some types of inhomogeneities, the stored energy for the homogeneous body that belong to the same class as the inhomogeneous body cannot describe the response of the body accurately.

Even though the variation of $(\mu_1)_{exp}$ with Ω is less than 10%, it is important to notice that the maximum deviation from the mean occurs for small values of Ω. For this class of deformations, when the inhomogeneity is periodic, say sinusoidal, increasing the frequency while keeping the amplitude fixed does not result in the homogenization becoming better. This is consistent with the observation of Saravanan and Rajagopal [21] for the Mooney solid.

6.3. Case 3: Pure Inflation

Finally, we consider the inflation of an annular right circular cylinder, held at a constant length, i.e. $\Omega = T_{rr}(r_o) = 0, \lambda = 1$. For this problem

$$\begin{aligned}
0.5\mathcal{P} &= \int_{R_i}^{R_o} \mu_1(R) \left[\left(\frac{r}{R}\right)^2 - r_{,R}^2\right] \frac{R}{r^2}\,\mathrm{d}R \\
&= (\mu_1)_{exp} \int_{R_i}^{R_o} \left[\left(\frac{r^*}{R}\right)^2 - r_{,R}^{*2}\right] \frac{R}{r^{*2}}\,\mathrm{d}R \\
(\mu_1)_{exp}^{Pr-Inf} &= \frac{\int_{R_i}^{R_o} \mu_1(R)[(\frac{r}{R})^2 - r_{,R}^2]\frac{R}{r^2}\,\mathrm{d}R}{\int_{R_i}^{R_o} [(\frac{r^*}{R})^2 - r_{,R}^{*2}]\frac{R}{r^{*2}}\,\mathrm{d}R} \qquad (123)
\end{aligned}$$

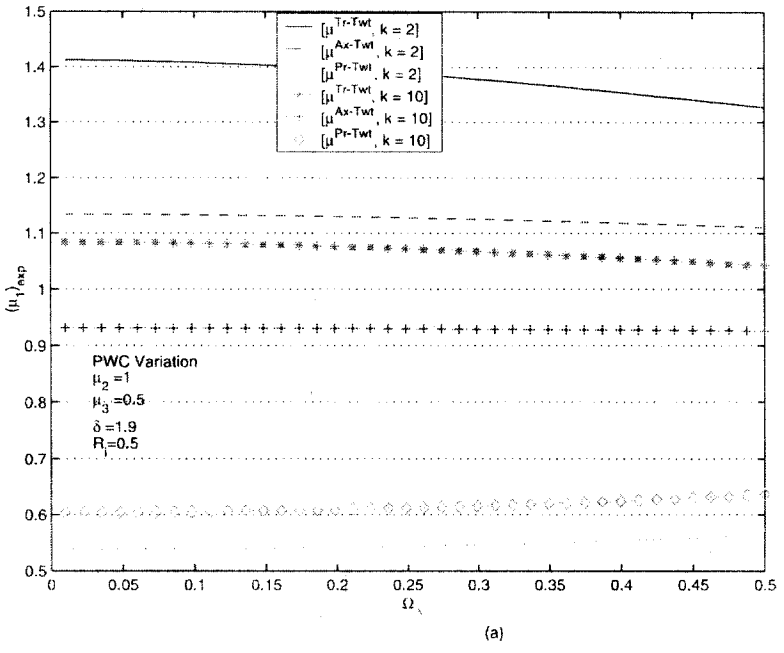

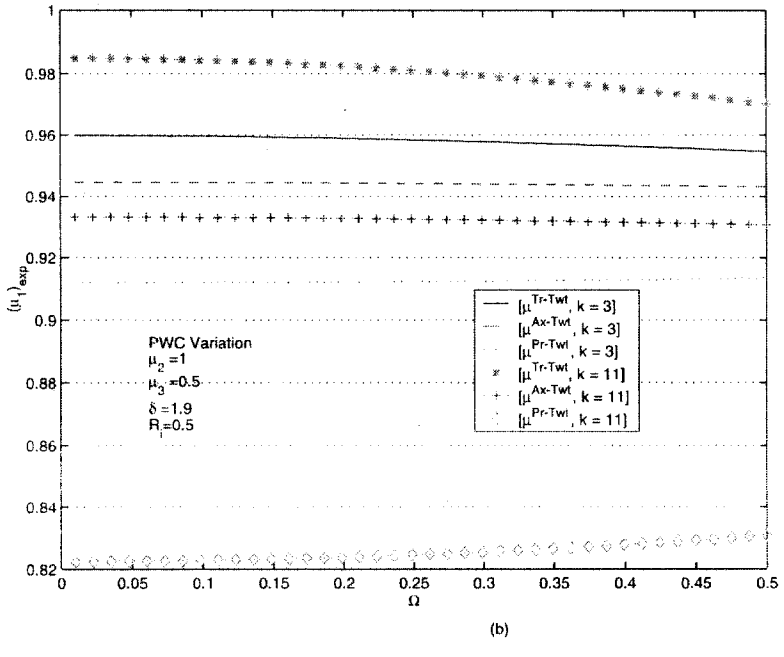

Figure 3. Plot of $(\mu_1)_{exp}$ vs Ω for various correlations when μ_2, μ_3 are constant and $\mu_1(\overline{R})$ = (a) $\delta + 2 * (1-\delta) * \sum_{n=0}^{k-1}(-1)^n H(\overline{R} - \frac{n}{k})$, (b) $\delta + 2 * (1-\delta)\frac{k}{(k+1)} \sum_{n=0}^{k-1}(-1)^n H(\overline{R} - \frac{n}{k})$.

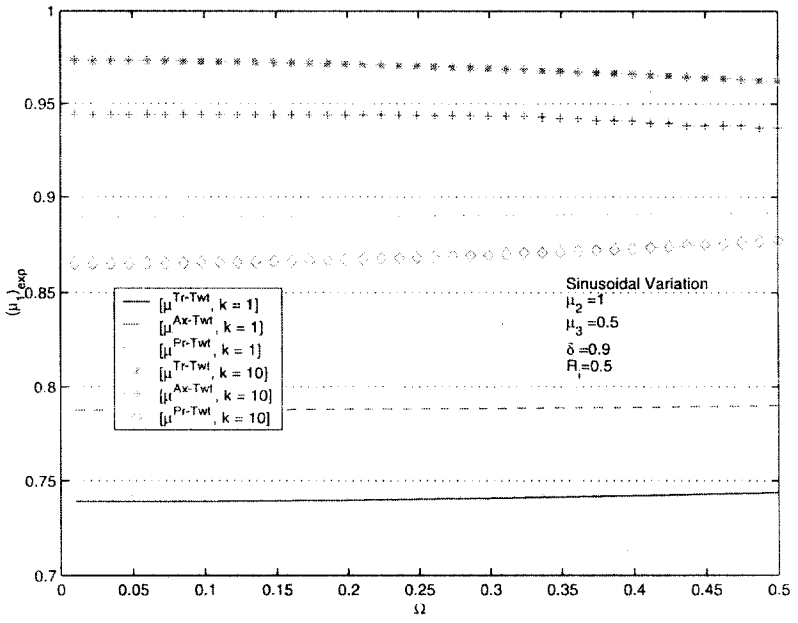

(a)

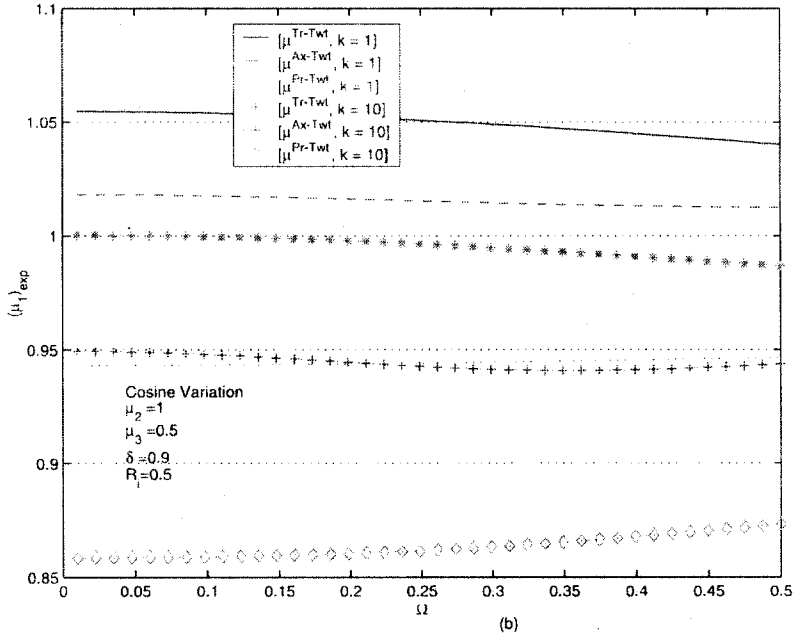

(b)

Figure 4. Plot of $(\mu_1)_{exp}$ vs Ω for various correlations when μ_2, μ_3 are constant and $\mu_1(\overline{R})$ = (a) $1 + \delta * \sin(2k\pi\overline{R})$ (b) $1 + \delta * \cos(2k\pi\overline{R})$.

from (118). As in the previous case, we can correlate the axial load required to maintain $\lambda = 1$ for a given r_i. Then

$$\begin{aligned}
\frac{(\mathcal{L}(r_i) - L_p(r_i))}{2\pi} &= \int_{R_i}^{R_o} \mu_1(R)\left[2 - r_{,R}^2 - \left(\frac{r}{R}\right)^2\right] R\,\mathrm{d}R, \\
&= (\mu_1)_{exp} \int_{R_i}^{R_o} \left[2 - r_{,R}^{*2} - \left(\frac{r^*}{R}\right)^2\right] R\,\mathrm{d}R, \\
(\mu_1)_{exp}^{Ax-Inf} &= \frac{\int_{R_i}^{R_o} \mu_1(R)[2 - r_{,R}^2 - (\frac{r}{R})^2]R\,\mathrm{d}R}{\int_{R_i}^{R_o} [2 - r_{,R}^{*2} - (\frac{r^*}{R})^2]R\,\mathrm{d}R}. \qquad (124)
\end{aligned}$$

Figures 5 and 6 capture the variation $(\mu_1)_{exp}$ obtained for this case with the value of r_i/R_i. We find that for this case the value of $(\mu_1)_{exp}$ could vary by as much as 30% and the maximum deviation from the mean occurs for small values of r_i/R_i. Thus, small deformations do not necessarily ensure robustness of the homogenization. Further, for this class of deformations, if the inhomogeneity is periodic, then increasing the frequency, while keeping the amplitude fixed, does not always result in the homogeneous approximation becoming better.

Figures 7–9 capture the variation of $(\mu_1)_{exp}$ with R_i for the various correlations considered above, for a given $\mu_1(R)$. We have once again assumed μ_3 to be a constant. Here $\lambda = 1.2, \Omega = 0.1, r_i = 1.3 * R_i$ for the respective cases.

We immediately recognize that the value of $(\mu_1)_{exp}$

(1) depends on the thickness of the cylinder;
(2) depends on the specific experiment used for the correlation.

Such characteristics are not desirable. Further, if the inhomogeneous Blatz–Ko body is made up of layers of homogeneous Blatz–Ko bodies with different material moduli (μ_1) varying about a mean, then one might believe that it could be modelled by a homogeneous Blatz–Ko body. The above results show that not to be the case. We find that increasing the frequency (k), keeping the amplitude (δ) fixed need not always result in the homogenization being better, as in the case of a Mooney solid.

Instead of homogenizing in the above manner, we can mathematically seek the constant value of the material parameter μ_1 associated with the homogeneous approximation for the inhomogeneous body belonging to the same class, such that the total stored energy in the inhomogeneous and homogeneous body are the same. Then, if we denote by $(\mu_1)_{mth}$ this constant parameter associated with the homogenized body, we find that it is given by

$$(\mu_1)_{mth} = \frac{\int_{R_i}^{R_o} \mu_1(R)(J_3^{-2\mu_3} + J_1 - 4)\,\mathrm{d}R}{\int_{R_i}^{R_o} ((J_3^*)^{-2\mu_3} + J_1^* - 4)\,\mathrm{d}R}, \qquad (125)$$

where J_i^* denotes the invariant found from the solution of the identical BVP for the corresponding homogeneous body. Let $(\mu_1)_{mth}^{cs1}$, $(\mu_1)_{mth}^{cs2}$, $(\mu_1)_{mth}^{cs3}$ denote the values of

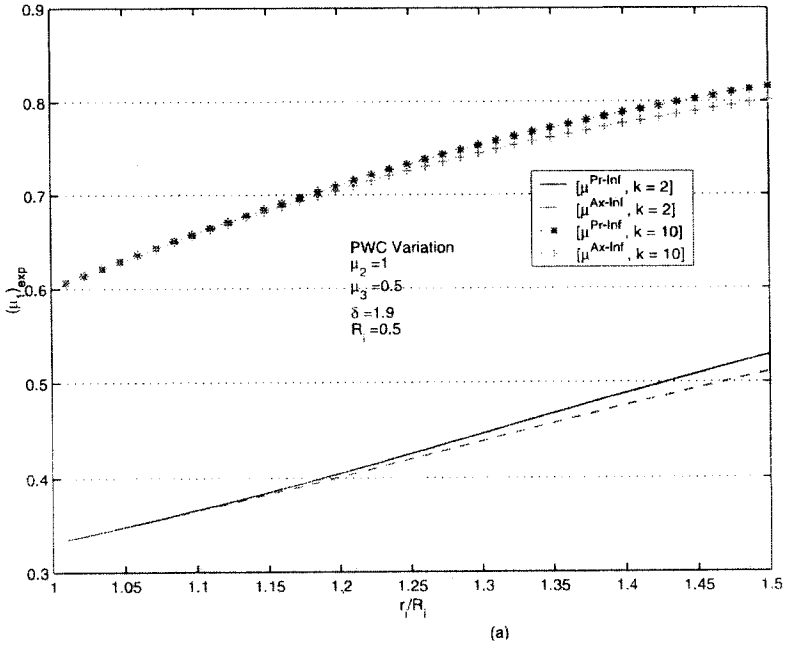

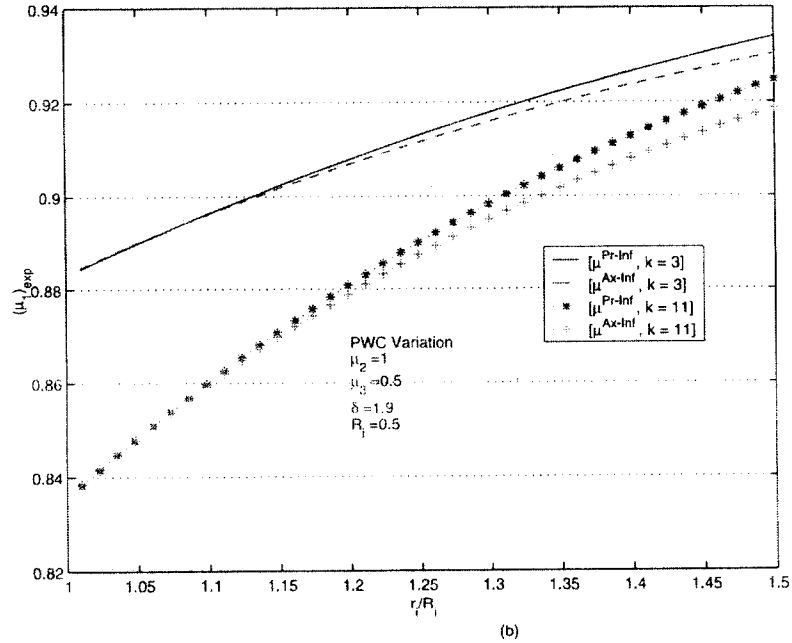

Figure 5. Plot of $(\mu_1)_{exp}$ vs r_i/R_i for various correlations when μ_2, μ_3 are constant and $\mu_1(\overline{R}) =$ (a) $\delta + 2 * (1-\delta) * \sum_{n=0}^{k-1}(-1)^n H(\overline{R} - \frac{n}{k})$, (b) $\delta + 2 * (1-\delta)\frac{k}{(k+1)}\sum_{n=0}^{k-1}(-1)^n H(\overline{R} - \frac{n}{k})$.

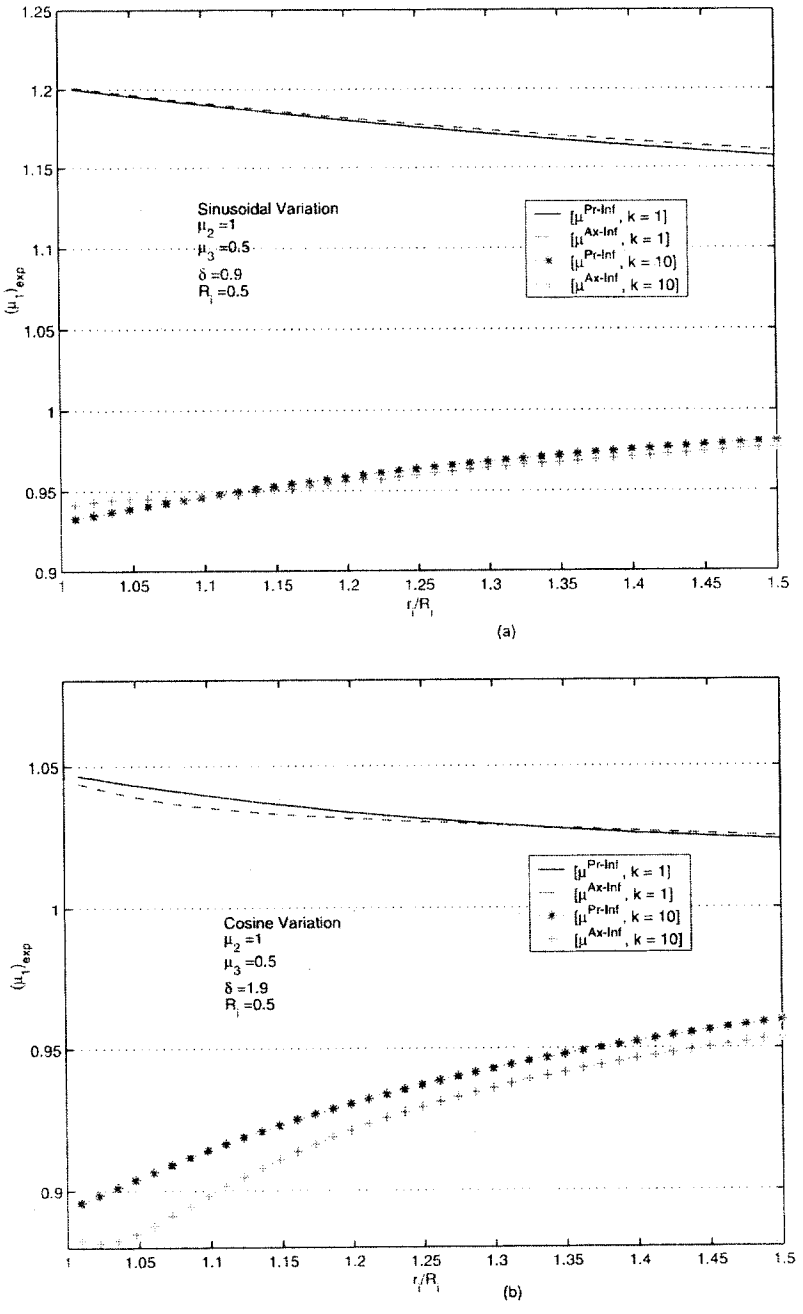

Figure 6. Plot of $(\mu_1)_{exp}$ vs r_i/R_i for various correlations when μ_2, μ_3 are constant and $\mu_1(\overline{R}) =$ (a) $1 + \delta * \sin(2k\pi\overline{R})$, (b) $1 + \delta * \cos(2k\pi\overline{R})$.

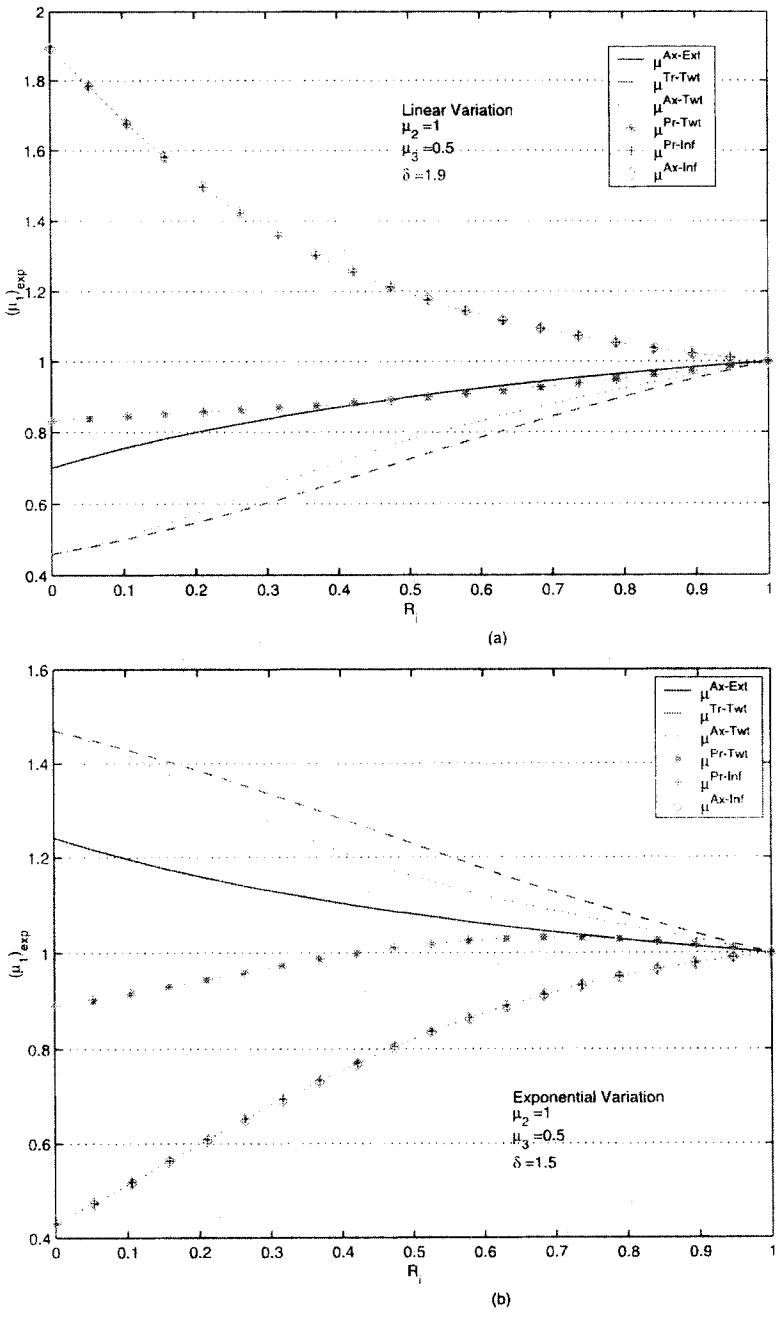

Figure 7. Plot of $(\mu_1)_{exp}$ vs R_i for various correlations when μ_2, μ_3 are constant and $\mu_1(\overline{R})$ = (a) $2(1-\delta)\overline{R}+\delta$, (b) $\frac{\delta}{(e^{\delta}-1)} * e^{\delta \bar{R}}$.

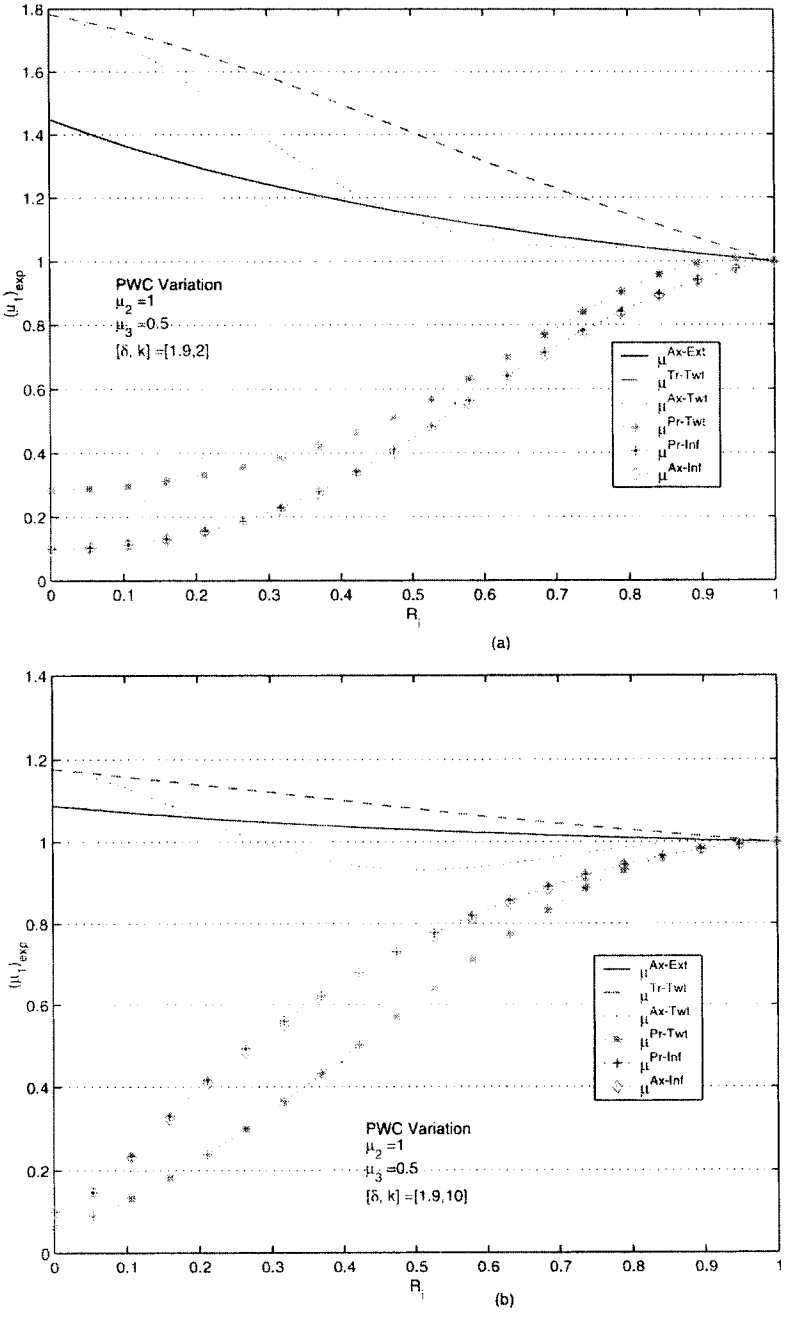

Figure 8. Plot of $(\mu_1)_{exp}$ vs R_i for various correlations when μ_2, μ_3 are constant and $\mu_1(\overline{R}) = \delta + 2 * (1 - \delta) * \sum_{n=0}^{k-1}(-1)^n H(\overline{R} - \frac{n}{k})$: (a) $k = 2$, (b) $k = 10$.

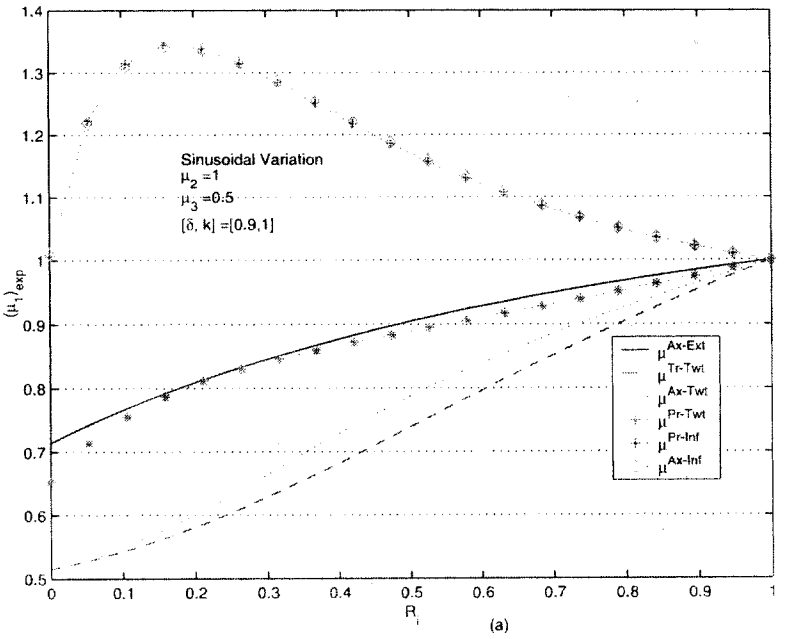

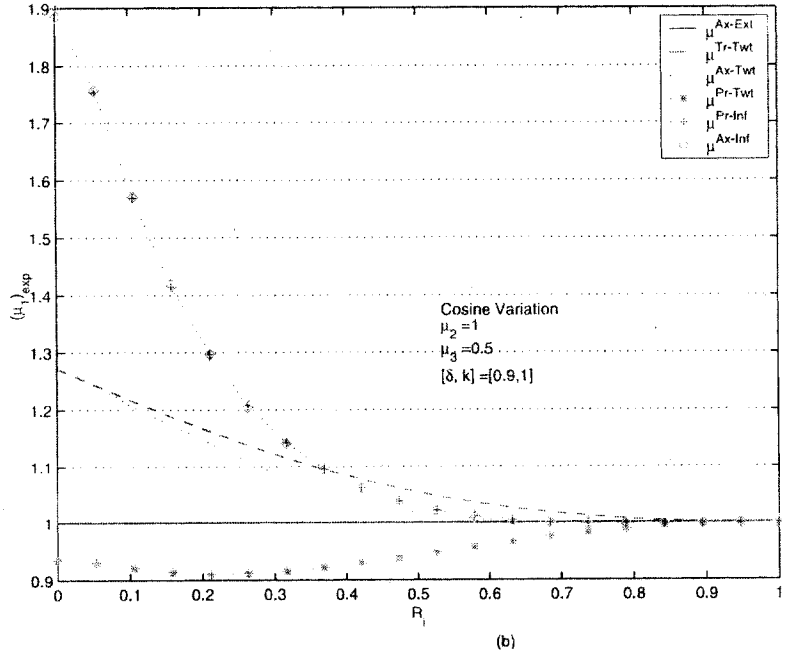

Figure 9. Plot of $(\mu_1)_{exp}$ vs R_i for various correlations when μ_2, μ_3 are constant and $\mu_1(\overline{R})$ = (a) $1 + \delta * \sin(2k\pi\overline{R})$ (b) $1 + \delta * \cos(2k\pi\overline{R})$.

$(\mu_1)_{mth}$ corresponding to the three BVPs studied earlier. The variation of $(\mu_1)_{mth}$ vs R_i is plotted in Figures 10–12. We have assumed μ_3 to be a constant and $\lambda = 1.2$, $\Omega = 0.1$, $r_i = 1.3 * R_i$ for the respective cases. Also, in these figures we have plotted the extreme values of μ_{exp} obtained, for the sake of comparison. It is evident that similar to $(\mu_1)_{exp}$, $(\mu_1)_{mth}$ also depends on Ω and r_i, indicating that the inhomogeneous body cannot be approximated by a homogeneous body with a stored energy function belonging to the same class.

It is not surprising that $(\mu_1)^{cs1}_{mth} = (\mu_1)_{mean}$ because when both the homogeneous and the inhomogeneous body allow for the same homogeneous deformation then it can be easily seen that $(\mu_1)_{mth} = (\mu_1)_{mean}$. This results in the under- or overestimation of the axial load by as much as 50%. It could be inferred from these figures that one cannot definitely say whether $(\mu_1)_{mth}$ underestimates or overestimates the required traction as this depends on the type of inhomogeneity under consideration (for example, if μ_1 monotonically increases or decreases) and the BVP. In any case, even for a given inhomogeneity, $(\mu_1)_{mth}$ (as also $(\mu_1)_{exp}$) *varies by as much as* 1800% depending on the BVP.

7. STRESS DISTRIBUTION

We now turn our attention to the differences between the stress distribution in the inhomogeneous solid and its homogeneous counterpart. It is not surprising that the stress distribution in the inhomogeneous body is quantitatively different from its homogeneous approximation. However, one would expect the qualitative aspects like the gradient of the stress or the sense of the stress to be preserved. Unfortunately, such is not the case and this was illustrated in the case of incompressible bodies by Saravanan and Rajagopal ([20, 21]). We also encounter a similar situation in the case of compressible bodies. This difference can have profound implications concerning the failure of the inhomogeneous body, calculations based on the homogeneous body proving to be useless or misleading.

Figures 13–15 show the stress distribution and $r(R)$ for various inhomogeneous bodies subjected to pure twist (case 2). Figures 16 and 17 provide the same for pure inflation (case 3). It can be easily seen from Figures 14a, 16b and 19 that the homogeneous approximation does not even predict the sense of stress correctly (compressive versus tensile) for these simple deformations.

Interestingly, for all the richness in the stress distribution, $r(R)$ is nearly identical for all types of inhomogeneities as seen from Figures 15a and 17a. However, Figures 15b and 17b show that the derivative of r in these problems is quite different. This also highlights the accuracy that the theory demands in the experimental observation to arrive at a robust stored energy function for an inhomogeneous body.

Figures 18–20 show how $r_{,R}$ and the transmural stress distribution vary when an inhomogeneous solid cylinder is uniaxially stretched. Here μ_3 alone is a function of R. Thus, the deformation of the cylinder is inhomogeneous. Also, note that $T_{rr} \neq 0$, $T_{\theta\theta} \neq 0$ in the case of an inhomogeneous cylinder. Figure 18a illustrates the accuracy required in experiments that track markers, an approach common in the testing of soft biological tissues, so that one could decide whether the deformation is homogeneous or otherwise.

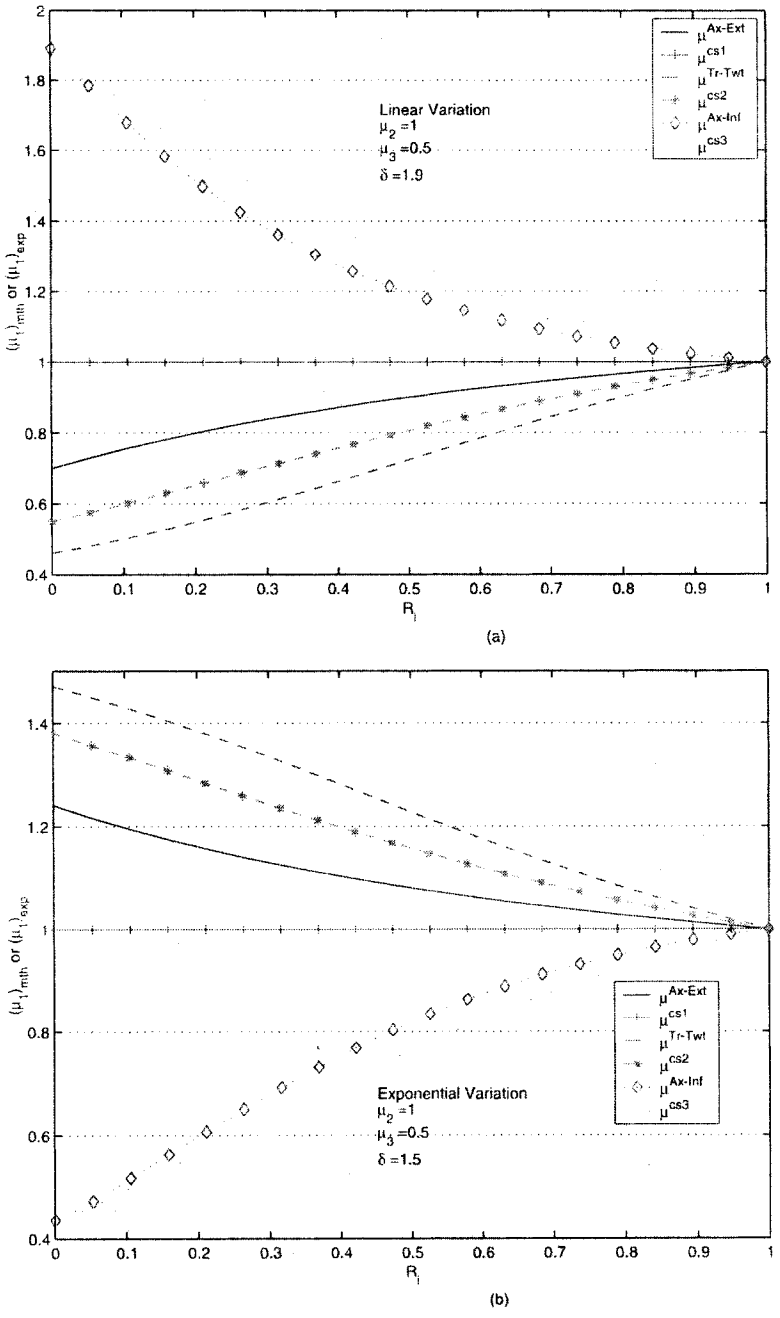

Figure 10. Plot of $(\mu_1)_{exp}$ or $(\mu_1)_{mth}$ vs R_i for various correlations when μ_2, μ_3 are constant and $\mu_1(\overline{R}) =$ (a) $2(1-\delta)\overline{R}+\delta$, (b) $\frac{\delta}{(e^{\delta}-1)} * e^{\delta \bar{R}}$.

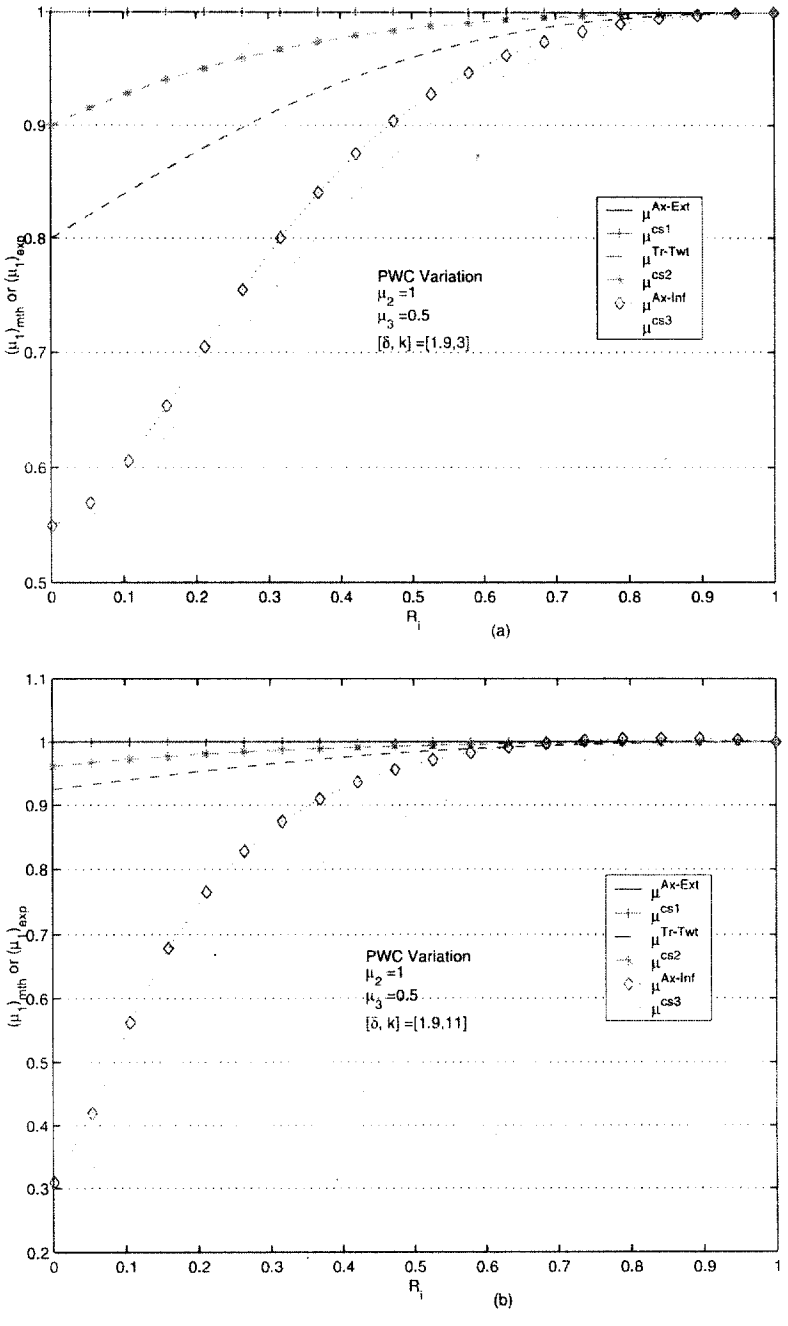

Figure 11. Plot of $(\mu_1)_{exp}$ or $(\mu_1)_{mth}$ vs R_i for various correlations when μ_2, μ_3 are constant and $\mu_1(\overline{R}) = \delta + 2 * (1-\delta)\frac{k}{(k+1)} \sum_{n=0}^{k-1} (-1)^n H(\overline{R} - \frac{n}{k})$: (a) $k = 3$, (b) $k = 11$.

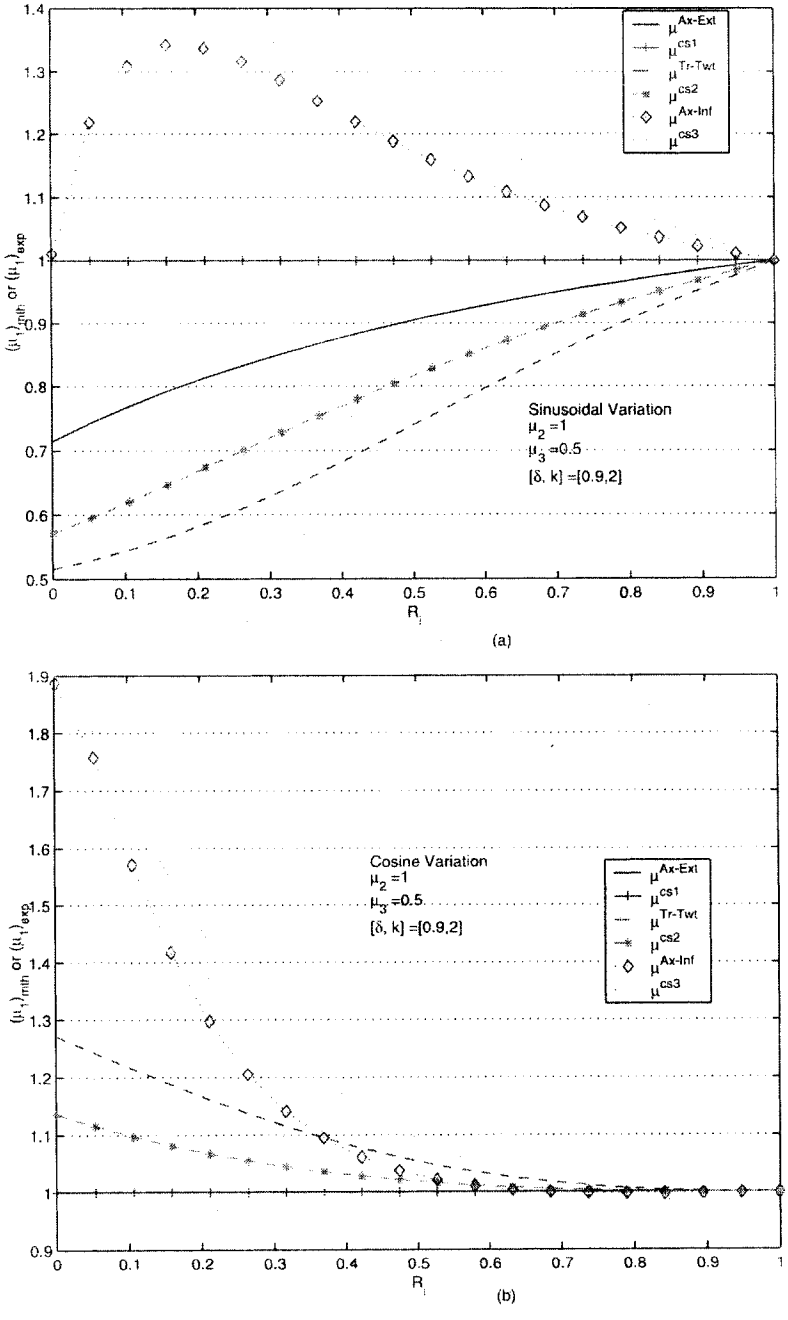

Figure 12. Plot of $(\mu_1)_{exp}$ or $(\mu_1)_{mth}$ vs R_i or $(\mu_1)_{mth}$ for various correlations when μ_2, μ_3 are constant and $\mu_1(\overline{R})$ = (a) $1 + \delta * \sin(2k\pi\overline{R})$, (b) $1 + \delta * \cos(2k\pi\overline{R})$.

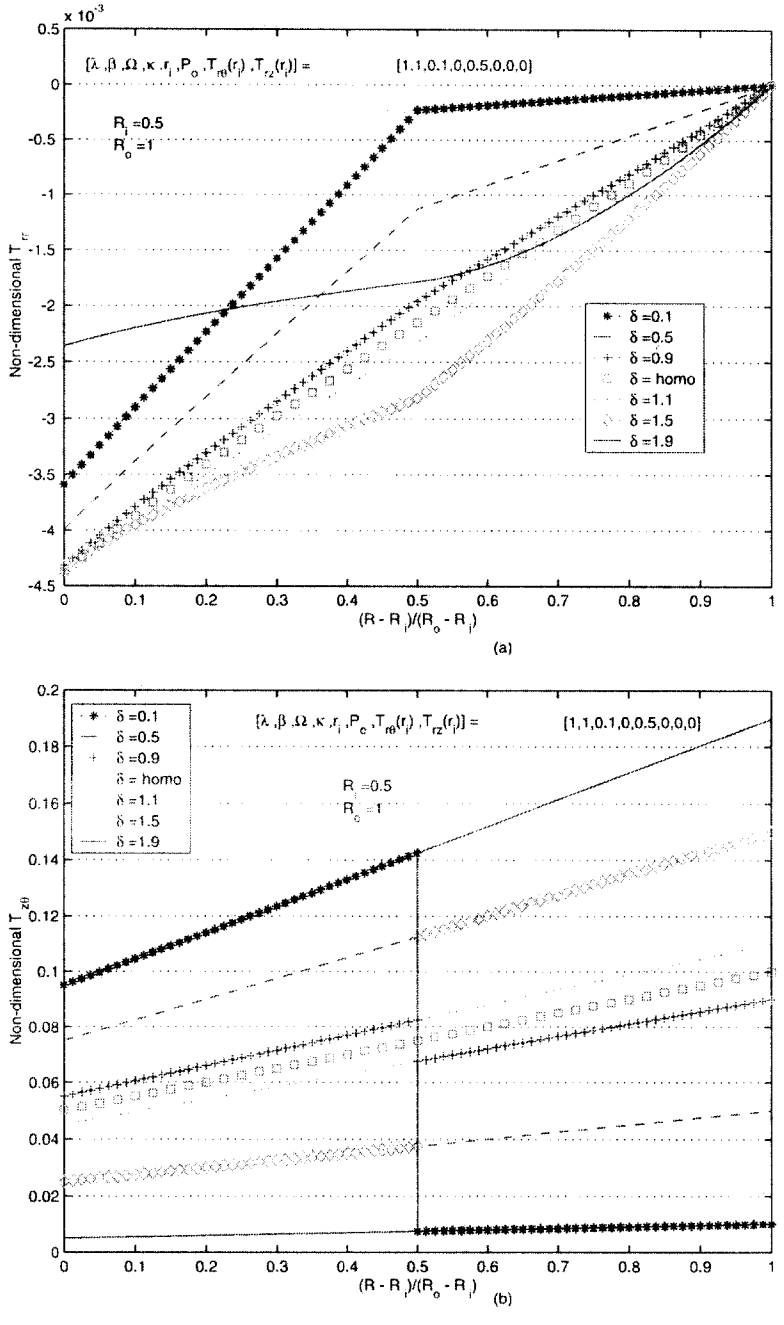

Figure 13. Plot of non-dimensional stress (a) T_{rr}, (b) $T_{z\theta}$ for an annular cylinder subjected to pure twist when $\mu_2(\overline{R}) = 1$, $\mu_3(\overline{R}) = 0.5$ and $\mu_1(\overline{R}) = \delta + 2 * (1 - \delta) * \sum_{n=0}^{k-1}(-1)^n H(\overline{R} - \frac{n}{k})$ when $k = 2$ for various values of δ.

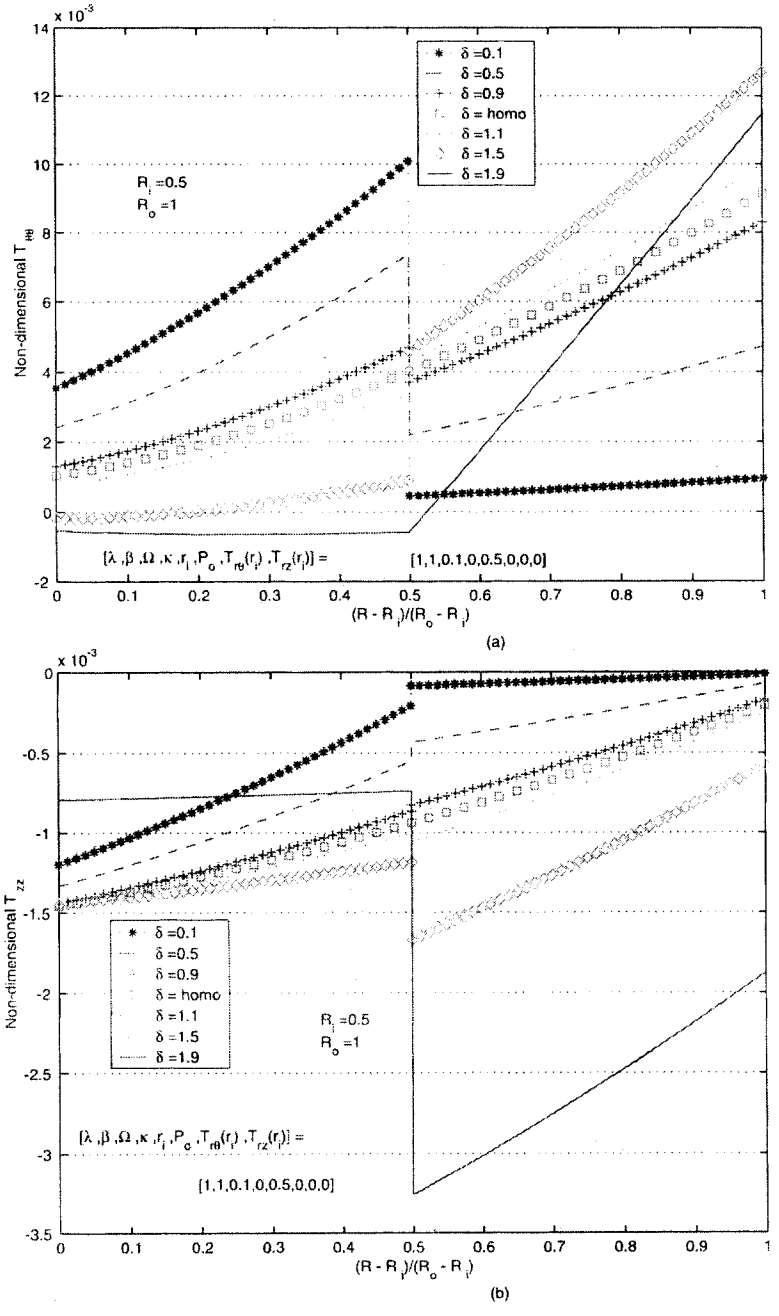

Figure 14. Plot of non-dimensional stress (a) $T_{\theta\theta}$, (b) T_{zz} for an annular cylinder subjected to pure twist when $\mu_2(\overline{R}) = 1$, $\mu_3(\overline{R}) = 0.5$ and $\mu_1(\overline{R}) = \delta + 2 * (1 - \delta) * \sum_{n=0}^{k-1}(-1)^n H(\overline{R} - \frac{n}{k})$ when $k = 2$ for various values of δ.

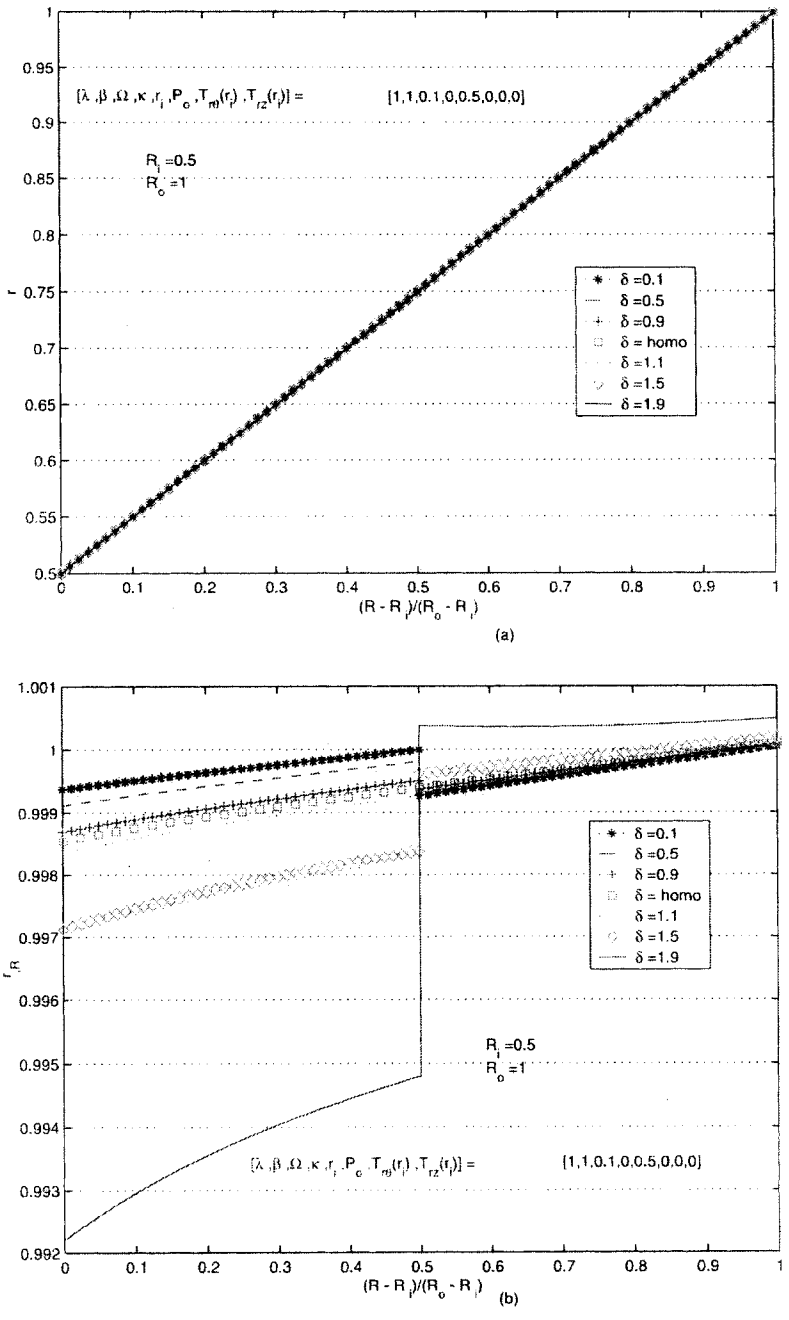

Figure 15. Plot of (a) $r(R)$, (b) $r_{,R}(R)$ for an annular cylinder subjected to pure twist when $\mu_2(\overline{R}) = 1$, $\mu_3(\overline{R}) = 0.5$ and $\mu_1(\overline{R}) = \delta + 2 * (1 - \delta) * \sum_{n=0}^{k-1}(-1)^n H(\overline{R} - \frac{n}{k})$ when $k = 2$ for various values of δ.

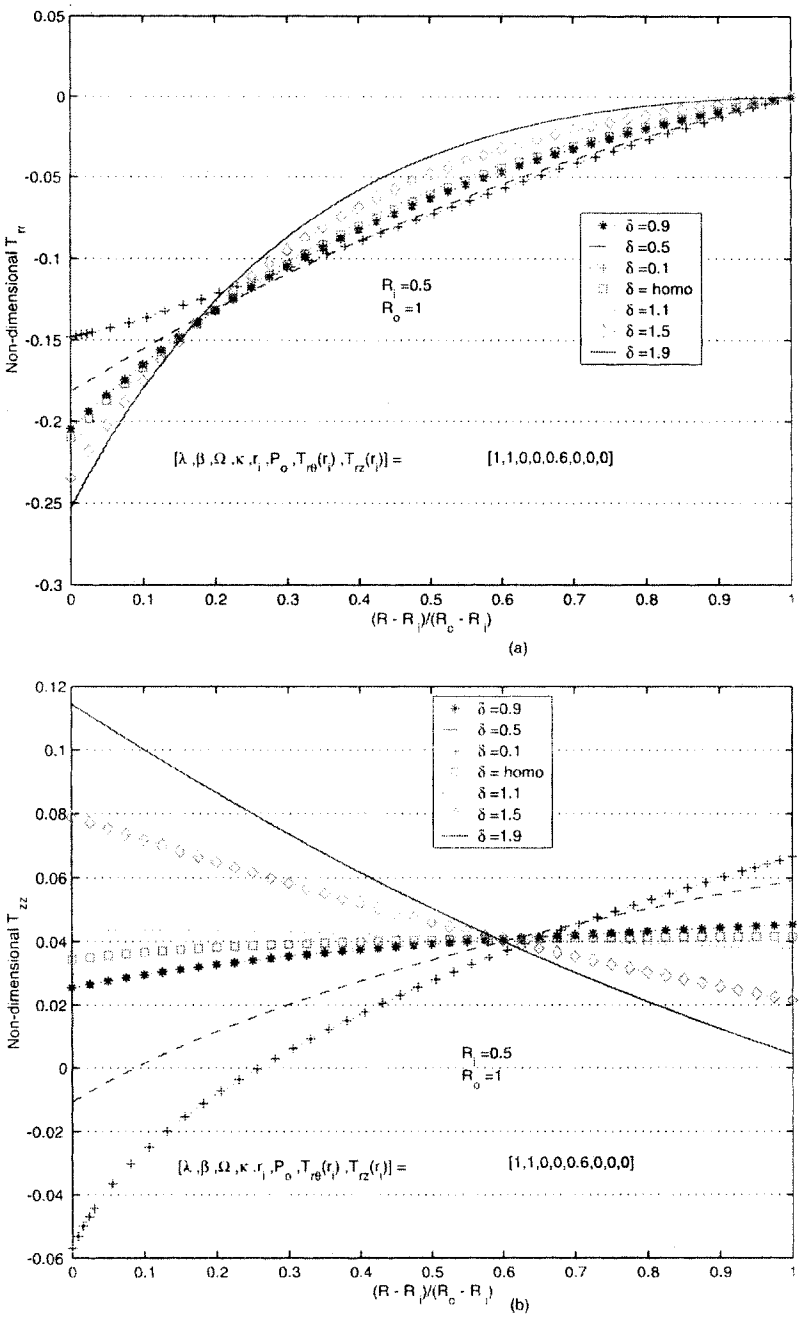

Figure 16. Plot of non-dimensional stress (a) T_{rr}, (b) T_{zz} for an annular cylinder subjected to pure inflation when $\mu_2(\overline{R}) = 1$, $\mu_3(\overline{R}) = 0.5$ and $\mu_1(\overline{R}) = 2(1-\delta)\overline{R} + \delta$ for various values of δ.

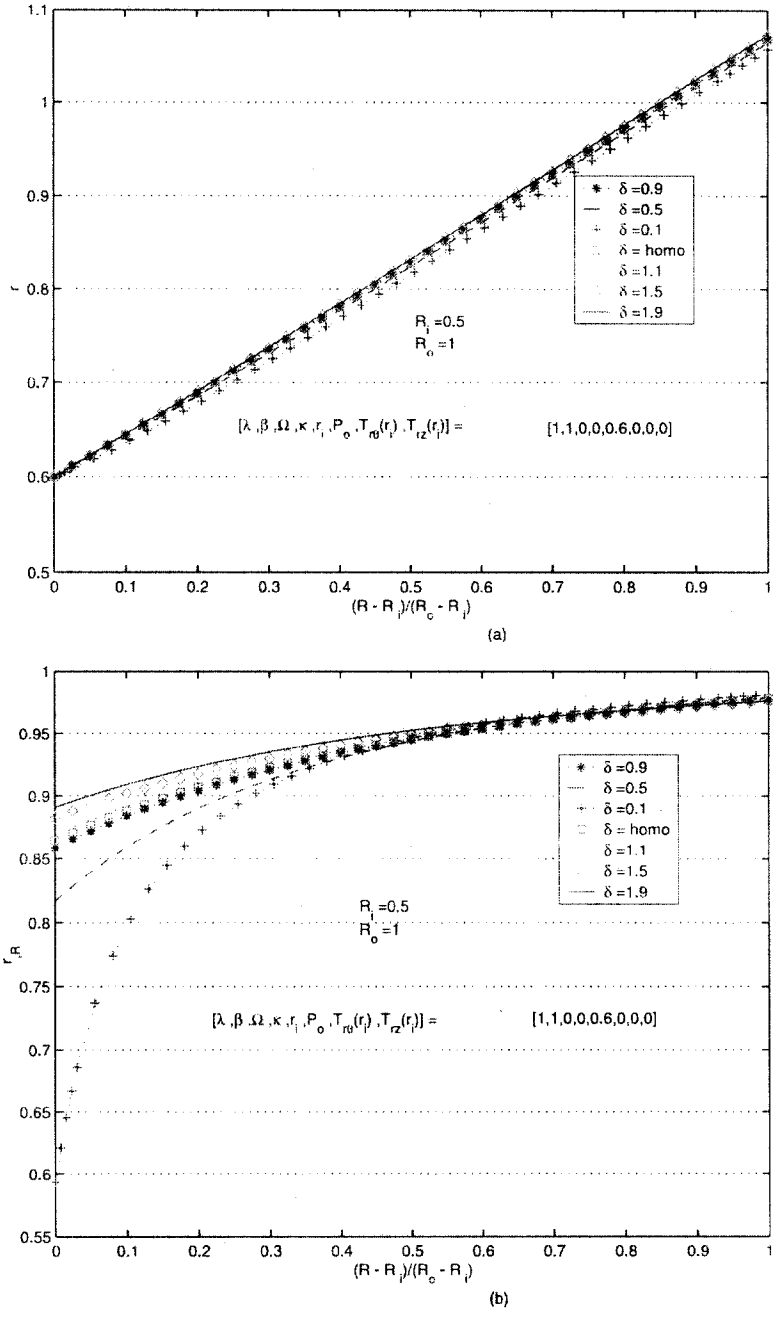

Figure 17. Plot of (a) $r(R)$, (b) $r_{,R}(R)$ for an annular cylinder subjected to pure inflation when $\mu_2(\overline{R}) = 1$, $\mu_3(\overline{R}) = 0.5$ and $\mu_1(\overline{R}) = 2(1-\delta)\overline{R} + \delta$ for various values of δ.

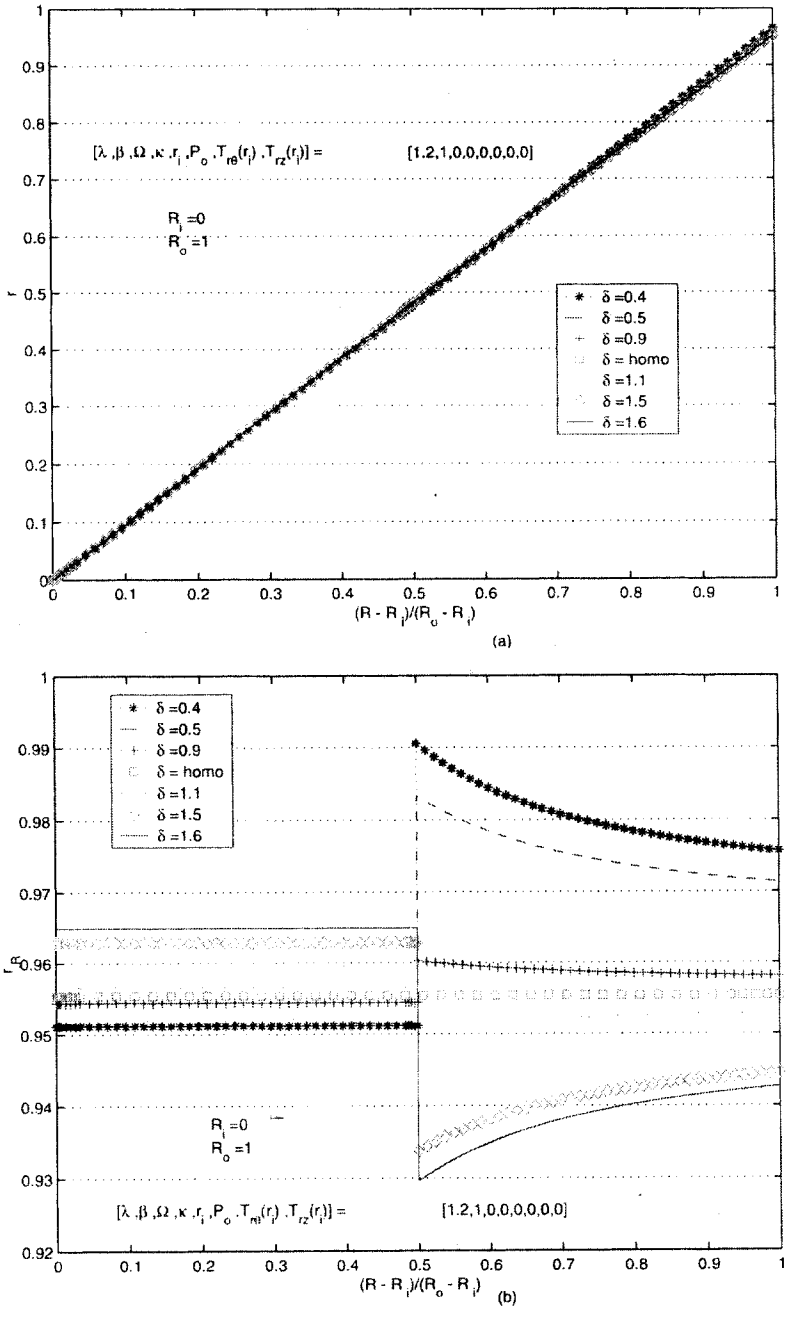

Figure 18. Plot of (a) $r(R)$, (b) $r_{,R}$ for a solid cylinder subjected to uniaxial extension when $\mu_1(\overline{R}) = 1$, $\mu_2(\overline{R}) = 1$ and $\mu_3(\overline{R}) = \delta + 2 * (1 - \delta) * \sum_{n=0}^{k-1} (-1)^n H(\overline{R} - \frac{n}{k})$ when $k = 2$ for various values of δ.

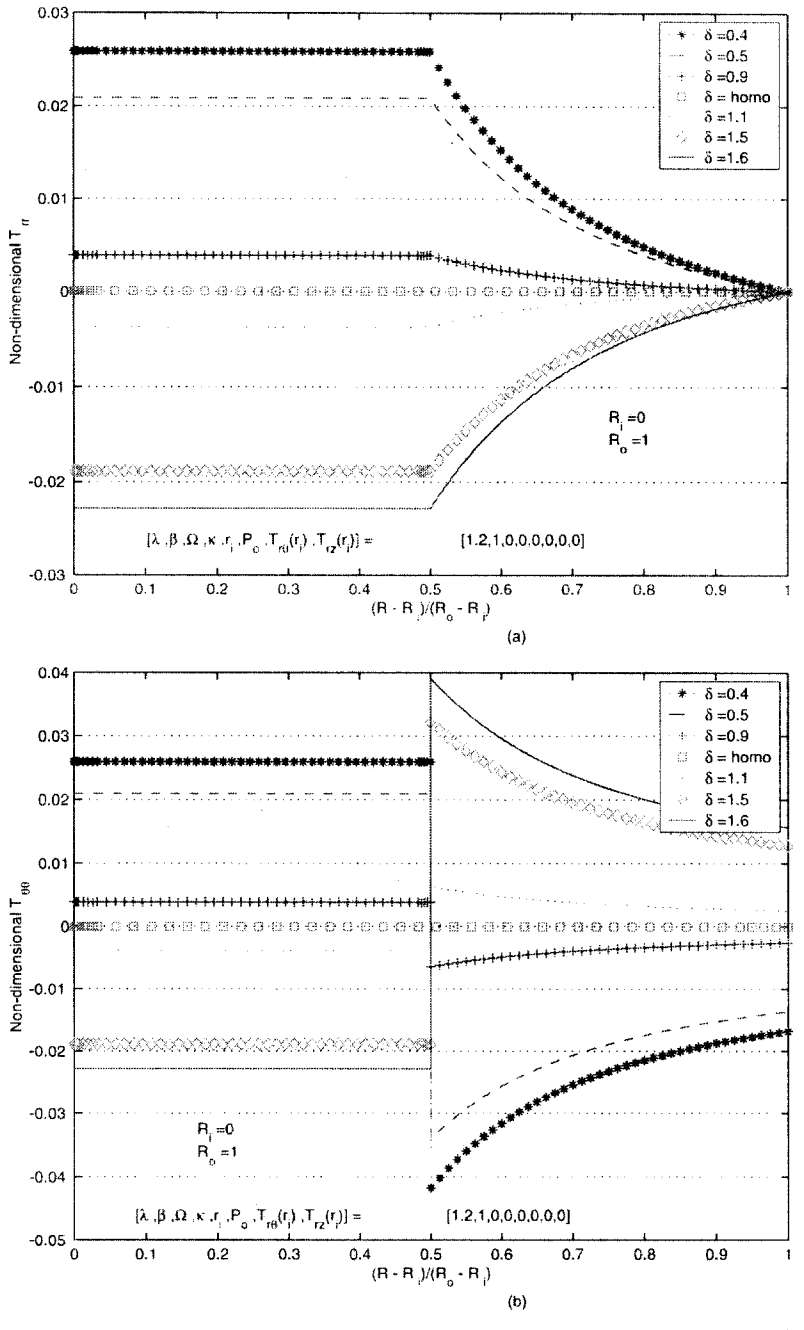

Figure 19. Plot of non-dimensional stress (a) T_{rr}, (b) $T_{\theta\theta}$ for a solid cylinder subjected to uniaxial extension when $\mu_1(\overline{R}) = 1$, $\mu_2(\overline{R}) = 1$ and $\mu_3(\overline{R}) = \delta + 2 * (1 - \delta) * \sum_{n=0}^{k-1}(-1)^n H(\overline{R} - \frac{n}{k})$ when $k = 2$ for various values of δ.

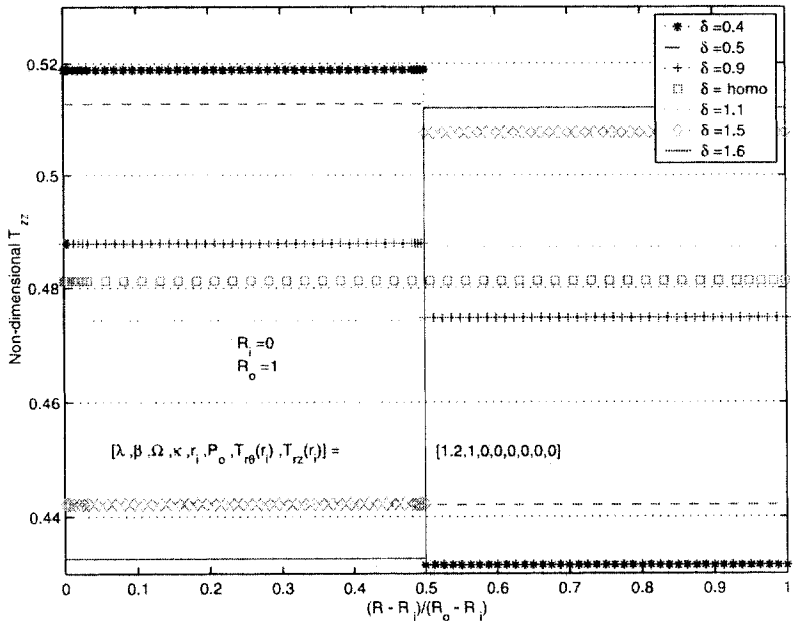

Figure 20. Plot of non-dimensional stress T_{zz} for a solid cylinder subjected to uniaxial extension when $\mu_1(\overline{R}) = 1$, $\mu_2(\overline{R}) = 1$ and $\mu_3(\overline{R}) = \delta + 2 * (1 - \delta) * \sum_{n=0}^{k-1}(-1)^n H(\overline{R} - \frac{n}{k})$ when $k = 2$ for various values of δ.

8. RESPONSE OF HOMOGENEOUS BLATZ–KO BODY

Here, we first consider the response of a thin cylinder to inflation at constant axial load and constant length as shown in Figure 21a. Clearly, the difference between these two responses increases as the radial inflation increases, even in the case of a thin cylinder. Figure 21b shows the torque versus twist response of a solid cylinder at constant load and constant stretch. It can be seen from the figure that changing the value of μ_2 has little effect on the solution. It can be observed that the radial component of the normal stress required to inflate the cylinder is less when unstretched in comparison to when unloaded irrespective of the value of μ_2. On the other hand, the torque required to engender a given twist is more at constant stretch ($\lambda = 1$) in comparison to constant axial load ($\mathcal{L} = 0$).

Next, we study the deformation corresponding to pure longitudinal shear, i.e. $[\beta, \kappa, \lambda, \Omega, T_{r\theta}(r_i), T_{rz}(r_i), P_o, r_i] = [1, 0, 1, 0, 0, 0, 0.1, R_i]$. Figures 22 and 23 capture the response of various classes of homogeneous bodies subjected to such a boundary condition. It can be seen from Figure 22a that, as observed by Polignone and Horgan [10], when $\mu_2 = 1$, $r = R$ is the solution to this problem. However, for other values of μ_2 one might be tempted to approximate the solution by $r = R$ by virtue of 22a. This is not a good approximation as the computed stresses will be erroneous as indicated by Figures 22b and 23, i.e. the stresses T_{rr} and $T_{\theta\theta}$ are non-zero.

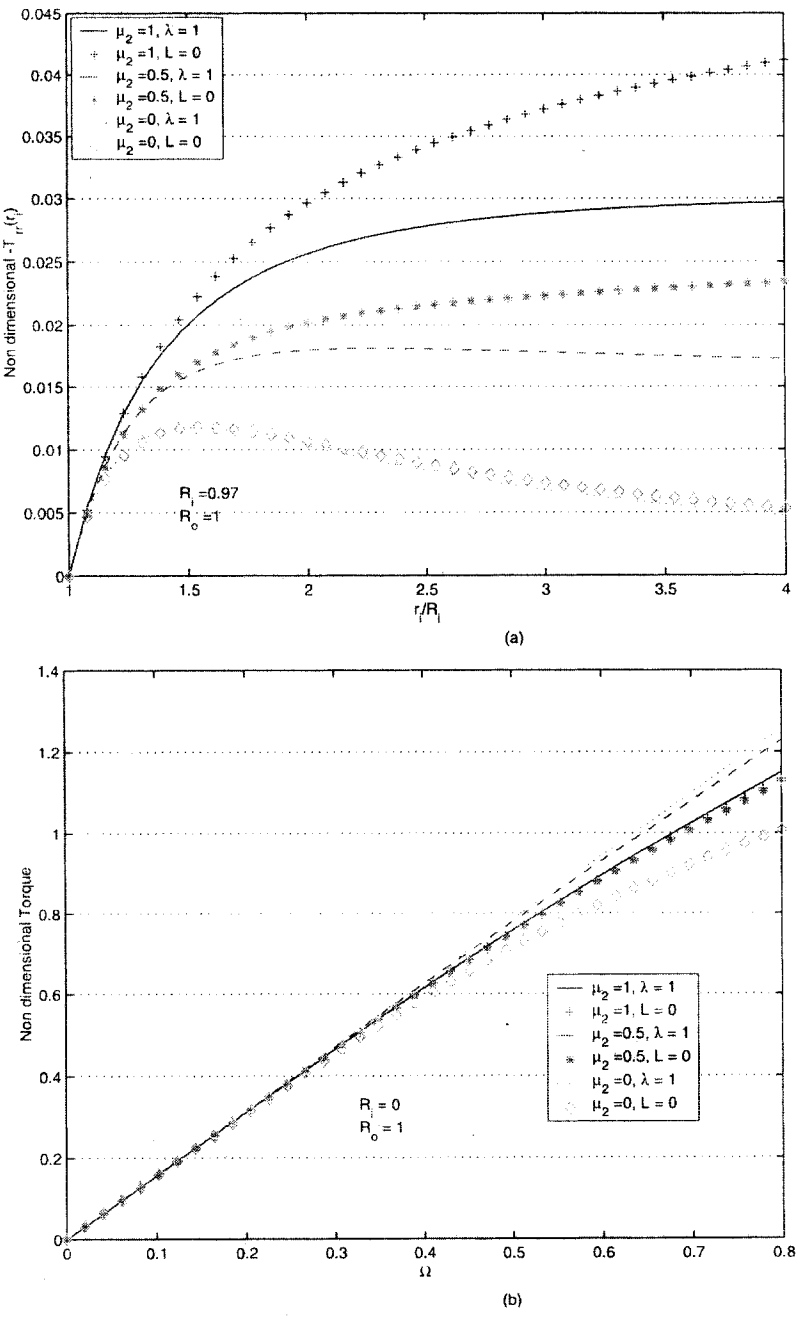

Figure 21. Plot of (a) non-dimensional stress $-T_{rr}(r_i)$ vs $\frac{r_i}{R_i}$, (b) non-dimensional torque vs Ω, when $\mu_1 = 1, \mu_3 = 0.5$ for various constant values of μ_2 under constant axial load ($L = 0$) and constant length ($\lambda = 1$).

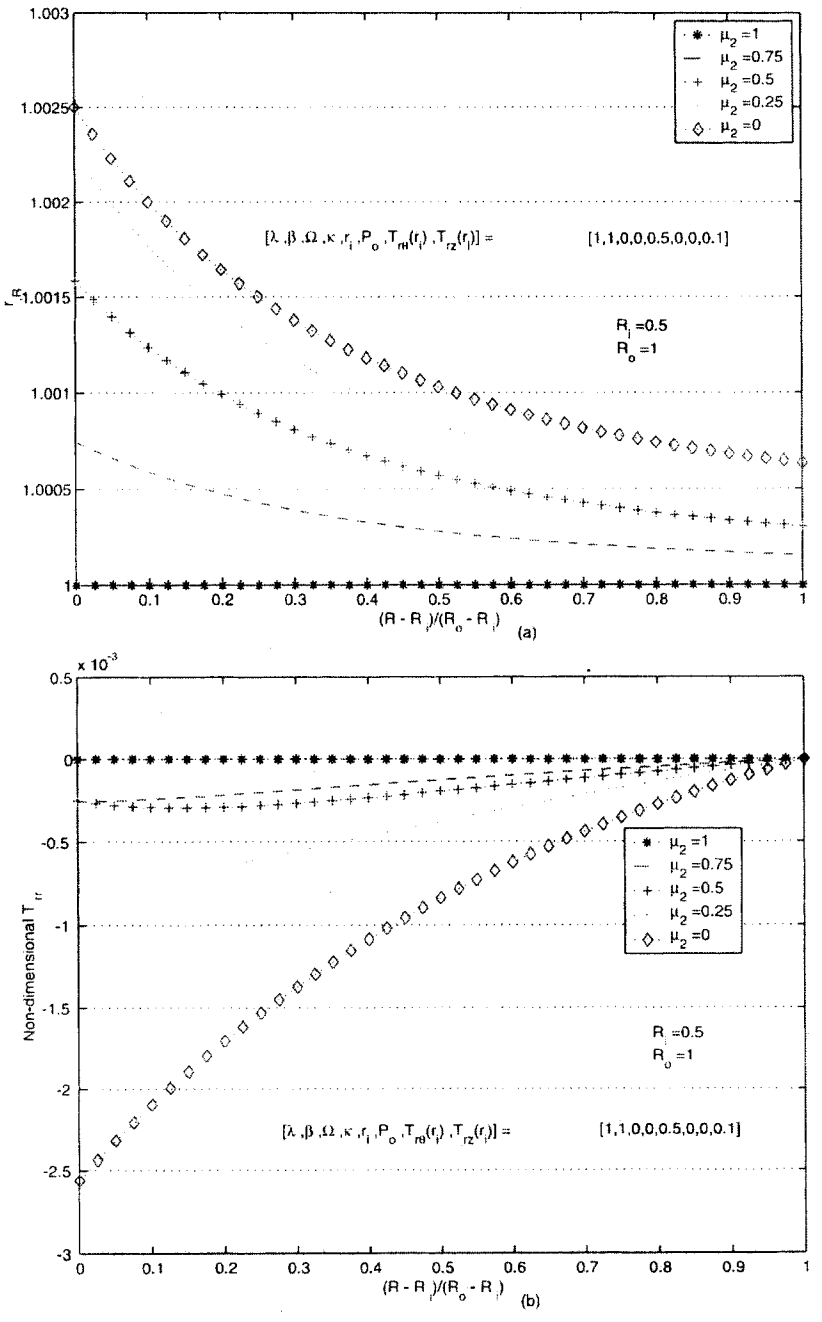

Figure 22. Plot of (a) $r_{,R}$, (b) non-dimensional stress T_{rr} when $\mu_1 = 1$ and $\mu_3 = 0.5$ for various constant values of μ_2 when [λ, β, Ω, κ, r_i, P_o, $T_{r\theta}(r_i)$, $T_{rz}(r_i)$] = $[1, 1, 0, 0, R_i, 0, 0, 0.1]$.

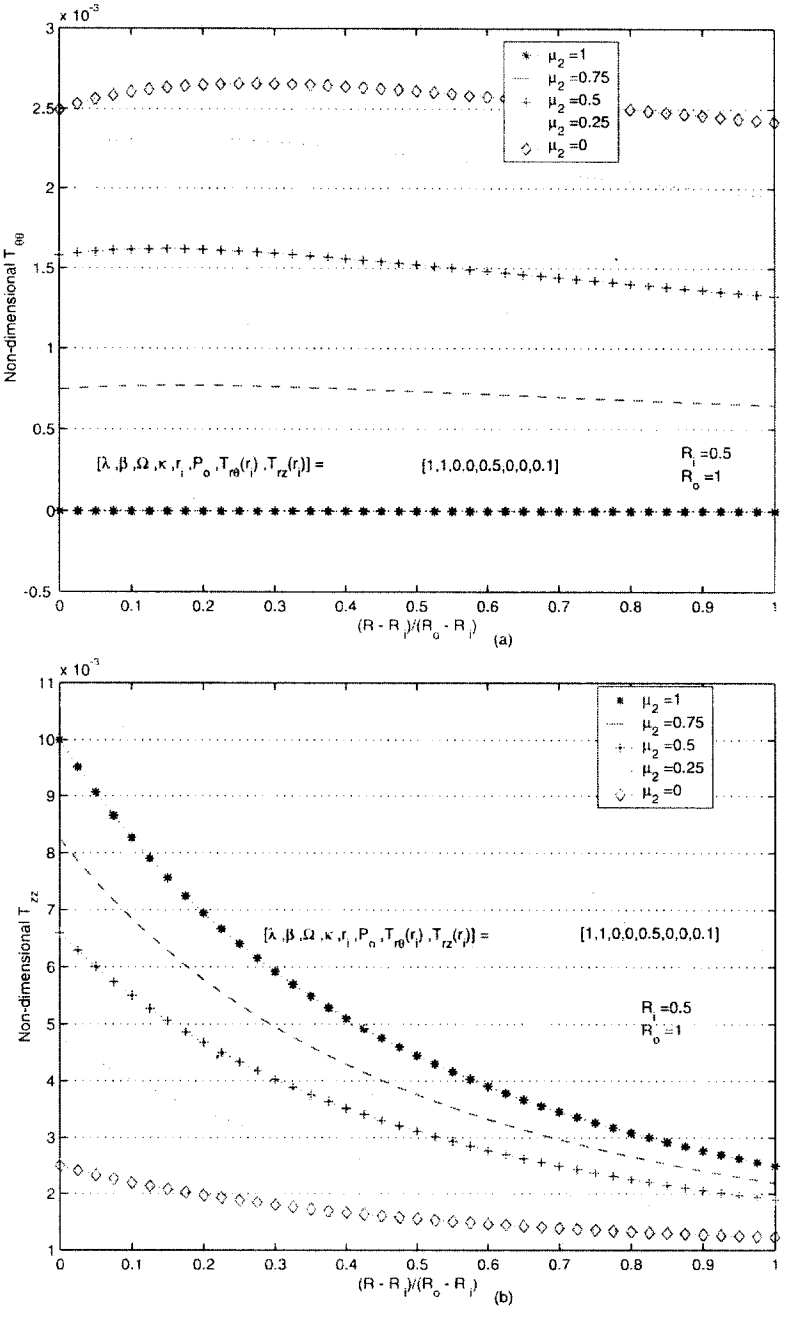

Figure 23. Plot of non-dimensional stress (a) $T_{\theta\theta}$, (b) T_{zz} when $\mu_1 = 1$ and $\mu_3 = 0.5$ for various constant values of μ_2 when [λ, β, Ω, κ, r_i, P_o, $T_{r\theta}(r_i)$, $T_{rz}(r_i)$] = $[1, 1, 0, 0, R_i, 0, 0, 0.1]$.

NOTE

1. Though it may be mathematically convenient to specify $r_{,R}(R_i)$ we specify the radial component of the normal stress at the outer surface, since in most instances we are interested in that value of $r_{,R}(R_i)$ which results in $P_o = 0$. We could easily determine $T_{rr}(r_i)$ from which we can obtain r_i for a given value of the radial component of the normal stress at the inner surface, if desired. Moreover, when $\mu_2 < 1$, $T_{rr}(r_i)$ is non-monotonic, resulting in the possibility of more than one solution.
2. Corresponding to each choice of $r_{,R}(0)$ there exists a value of $T_{rr}(r_o)$ and for each choice of λ there exists an axial load. Thus, if the required radial component of normal stress is applied at r_o, the value $r_{,R}(0)$ can be calculated.

Acknowledgement. We thank the National Institutes for Health and National Science Foundation for support of this work.

REFERENCES

[1] Truesdell, C. and Noll, W. The nonlinear field theories, in *Handbuch der Physik*, Vol. III/3, ed. S. Flügge, Springer, Berlin, 1965.

[2] Ericksen, J. L. Deformation possible in every compressible isotropic perfectly elastic material. *Journal of Mathematics and Physics,* 34, 126–128 (1955).

[3] Blatz, P. J. and Ko, W. L. Application of finite elastic theory to the deformation of rubbery materials. *Transactions of the Society of Rheology,* 6, 223–251 (1962).

[4] Knowles, J. K. and Sternberg, E. On the ellipticity of the equations of elastostatics for a special material. *Journal of Elasticity,* 5, 341–361 (1975).

[5] Beatty, M. F. Topics in finite elasticitiy: Hyperelasticity of rubber, elastomers, and biological tissues—with examples. *Applied Mechanics Review,* 40, 1699–1733 (1987).

[6] Wineman, A. S. and Waldron, W. K. Normal shear stress induced due to circular shear of a compressible non-linear elastic cylinder. *International Journal of Non-Linear Mechanics,* 30, 323–339 (1995).

[7] Chung, D. T., Horgan, C. O. and Abeyaratne, R. The finite deformation of internally pressurized hollow cylinders and spheres for a class of compressible elastic materials. *International Journal of Solids Structures,* 22, 1557–1570 (1986).

[8] Carroll, M. M. and Horgan, C. O. Finite strain solutions for a compressible elastic solid. *Quarterly of Applied Mathematics,* 48, 767–780 (1990).

[9] Polignone, D. A. and Horgan, C. O. Pure Torsion of compressible nonlineraly elastic circular cylinders. *Quarterly of Applied Mathematics,* 49, 591–607 (1991).

[10] Polignone, D. A. and Horgan, C. O. Axisymmetric finite anti-plane shear of compressible non-linearly elastic circular tubes. *Quarterly of Applied Mathematics,* 50, 323–341 (1992).

[11] Polignone, D. A. and Horgan, C. O. Pure azimuthal shear of compressible nonlinearly elastic tubes. *Quarterly of Applied Mathematics,* 52, 113–131 (1994).

[12] Mioduchowski, A. and Haddow, J. B. Combined torsional and telescopic shear of a compressible hyperelastic tube. *Journal of Applied Mechanics,* 46, 223–226 (1979).

[13] Zidi, M. Torsion and telescopic shearing of a compressible hyperelastic tube. *Mechanics Research Communication,* 26, 245–252 (1999).

[14] Zidi, M. Azimuthal shearing and torsion of a compressible hyperelastic and prestressed tube. *International Journal of Non-Linear Mechanics,* 35, 201–209 (2000).

[15] Zidi, M. Finite torsion and shearing of a compressible and anisotropic tube. *International Journal of Non-Linear Mechanics,* 35, 1115–1126 (2000).

[16] Hill, R. On constitutive macro-variables for heterogeneous solids at finite strain. *Proceedings of the Royal Society of London* A, 326 131–147 (1972).

[17] Eshelby, J. D. The determination of the elastic field of an ellipsoidal inclusion and related problems. *Proceedings of the Royal Society of London* A, 241, 376–396 (1957).

[18] Imam, A., Johnson, G. C. and Ferrari, M. Determination of the overall moduli in second order incompressible elasticity. *Journal of Mechanics and Physics of Solids,* 43, 1087–1104 (1995).

[19] Bolzon, G. and Vitaliani, R. The Blatz–Ko material model and homogenization. *Archive of Applied Mechanics,* 63, 228–241 (1993).

[20] Saravanan, U. and Rajagopal, K. R. On the role of inhomogeneities in the deformation of an elastic body. *Mathematics and Mechanics of Solids*, 8, 349–376 (2003).

[21] Saravanan, U. and Rajagopal, K. R. A comparison of the response of isotropic inhomogeneous elastic cylindrical and spherical shells and their homogenized counterparts, *Journal of Elasticity* 71, 205–233 (2003).

[22] Castañeda, P. P. and Tiberio, E. A second-order homogenization method in finite elasticity and applications to back-filled elastomers. *Journal of the Mechanics and Physics of Solids,* 48, 1389–1411 (2000).

[23] Horgan, C. O. Remarks on ellipticity for the Generalized Blatz–Ko constitutive model for a compressible nonlinearly elastic solid. *Journal of Elasticity,* 42, 165–175 (1996).

[24] Saravanan, U. A study on the isothermal elastic response of inhomogeneous materials for certain classes of boundary value problems. *M.Sc. Thesis*, Department of Mechanical Engineering, Texas A&M University, College Station, TX (2001).